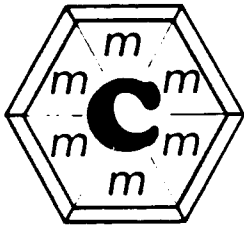# 9950 - 1296

JPL-IN-76-CR

80589

79P.

THE

MATHEMATICS CLINIC

MODELLING SHORT CHANNEL MOSFETS
FOR USE IN VLSI

By

Alex Klafter
Stuart Pilorz
Rosa Loguercio Polosa
Guy Ruddock (Team Leader)
Andrew Smith (Fall)

Professor Mario Martelli, Faculty Supervisor
Professor Ellis Cumberbatch, Faculty Consultant

FINAL REPORT

TO

JET PROPULSION LABORATORY

MAY 1986

Contract No. 957377

TABLE OF CONTENTS

I. Introduction

This is the second year of the JPL - sponsored Mathematics Clinic at CGS concerned with the metal-oxide-semiconductor-field-effect-transistor (MOSFET), in addition to the 1984 summer project. The primary focus of last year's Clinic was to obtain values of various device parameter constants used in one-dimensional (1-D) current models from data supplied by JPL ("parameter extraction"), and so the work was numerical in nature.

The goal of this year's MOSFET clinic was to deliver to JPL a mathematical model of the device dynamics from which an accurate and computationally efficient drain current expression could be derived for subsequent parameter extraction purposes. The initial plan was to obtain a simple 2-D model. However, a careful study of several 1-D models (see [2], [3], [4], [7], [11]) revealed many weak points in their derivation. Moreover no one of them included an analysis of the source and drain regions. Consequently the team decided to look for a more "acceptable" 1-D model, namely one whose derivation did not include procedures and approximations which we could not justify, and in which the role of the source and drain regions would be incorporated. At the same time we wanted to provide a comparison of the 1-D models previously mentioned together with some explanation of their failure to provide accurate drain current values at V_{GS} ≤ 2 and $V_{BS} \leq -3$ (phenomena that were detected by last year's clinic). We feel that all these goals have been achieved.

The 1-D model provided in 3.4 is mathematically sound and satisfactory. It allows the source and drain to operate in different regimes; it is not based on a questionable derivation of the depth of the depletion layer and it includes the contribution of current from the pinched-off part of the device, a feature not seen in any of the previous models.

The analysis of source and drain regions of 4.2, 4.3, although not entirely original is assembled here for the first time. The resistances R_S and R_D of the source and drain regions are estimated and used in 4.4 to evaluate the potentials Φ_{S0} and Φ_{SL} at the source and drain end of the channel respectively:

$$\Phi_{S0} = R_S I$$
$$V_{DS} - \Phi_{SL} = R_D I .$$

There are reasonable doubts that $R_S I$ and $R_D I$ may be related to the quasi-Fermi level for electrons at the source and at the drain more than to Φ_{S0} and Φ_{SL} . Future investigation is needed to decide their proper place in the current expression.

The qualitative and quantitative comparison of 5.1 - 5.5 will provide JPL with a useful quick-reference analysis of the most celebrated long-channel models, from the Pao-Sah double integral formula to the Brews [2], [3] and Wiele [11] closed-form current expression. No extensive introduction to these previous models will be made here; reference will be made to the 1984 summer report [5] by Morris-Everson and to the comprehensive book by Sze [10].

We conclude with the list of symbols and notations (Appendix 1) used in the report and a comparative list of them (Appendix 2) as used by the referenced authors.

II. CHANNEL MODELLING

2.1 Charge Distribution

Estimation of the number of electrons in the inversion layer at any
point along the channel is essential to an accurate evaluation of the current
at that point. The number may be given by the statistical mechanical distri-
bution dependent upon potential and thermal energy. One assumes the Fermi-
level to lie somewhere within the forbidden region, and that there will
be few enough conduction electrons that the Boltzman approximation to the
Fermi-distribution may be used. Within the bulk one applies the law of
mass action to obtain that the product of free carriers will be a constant,
dependent only upon temperature. That is,

$$2.1.1 \qquad np = n_i^2 \quad .$$

Assuming that for p-type material the number of positive ion impurities
is much greater than negative impurities, $N_A \gg N_D$, we approximate

$$2.1.2 \qquad N_A \approx n_i e^{\beta \phi_F} \quad ,$$

and

$$2.1.3 \qquad N_D N_A = n_i^2 \quad .$$

Here N_A and N_D are estimated concentrations. In formulating distributions
for free holes and electrons, we assume that for a p-type semiconductor,
the holes (being the majority carrier) feel no effects due to the local quasi-
Fermi level, so that

$$2.1.4 \qquad \phi_p = \phi_F$$

and

2.1.5a $\qquad p = n_i e^{-\beta(\phi - V_{BS} - \phi_F)}$,

2.1.5b $\qquad n = n_i e^{\beta(\phi - V_{BS} - \phi_n)}$,

where all potentials are in volts.

The inclusion of the body-to-source potential in these distributions is to account for the fact that the Fermi-level will be adjusted downwards following the application of negative potentials to the body. The inclusion of a quasi-Fermi level for electrons allows for variation in electron distribution along the channel, such that the relative (and complementary) percentages of current due to drift and diffusion may change. The quasi-Fermi level is assumed to lie within the interval

2.1.6 $\qquad \phi_F - V_{BS} < \phi_n < \phi_F - V_{BS} + V_{DS}$.

The left hand side represents the value of ϕ_n at the source end of the channel, while the right hand side represents its value at the drain end. Hence

2.1.7

$$n = n_i e^{\beta(\phi - \phi_F)} \qquad \text{at the source} \qquad ,$$

$$n = n_i e^{\beta(\phi - \phi_F - V_{DS})} \qquad \text{at the drain} \qquad .$$

This allows for variation of the channel potential dependent upon the potential applied to the drain, V_{DS}. The electron concentration is assumed to be negligible at any point in the channel when the exponent in (2.1.5b)

becomes zero (see 3.4). For every $y \in [0,L]$, where L is the length of the channel, we obtain a value $x(y)$ at which $\phi = \phi_n + V_{BS}$. This value represents the depth of the inversion layer at least in certain regimes of operation (see 3.4 for additional details).

2.2 Poisson's Equation and Surface Potential

Using the charge distribution of 2.1 we can formulate a partial differential equation satisfied by the electric potential ϕ. Since we are interested only in the stationary state, Maxwell's equations are reduced to the single Poisson's equation

$$2.2.1 \qquad \text{div}(\varepsilon_s \nabla \phi) = \rho$$

where ε_s is the semiconductor permittivity and ρ is the charge density. In our case we have

$$2.2.2 \qquad \rho = q(n - p + N_A^- - N_D^+)$$

where N_A^- and N_D^+ are the ionized acceptors and donors respectively. Using (2.1.5a), (2.1.5b) and the assumption that charge neutrality must exist in the bulk of the device we obtain

$$2.2.3 \qquad \rho = qn_i(e^{\beta(\phi - \phi_n - V_{BS})} - e^{-\beta(\phi - \phi_F - V_{BS})} + e^{\beta\phi_F} - e^{-\beta\phi_F})$$

where n_i is the intrinsic carrier concentration.

If we assume that ε_s is position independent (homogeneous material) we obtain from (2.2.1) and (2.2.3)

$$2.2.4 \qquad \Delta\phi = \frac{qn_i}{\varepsilon_s}(e^{\beta(\phi - \phi_n - V_{BS})} - e^{-\beta(\phi - \phi_F - V_{BS})} + e^{\beta\phi_F} - e^{-\beta\phi_F}) \quad .$$

If the variables x,y,z are used to denote the depth, length and width of the device respectively we have that ϕ is independent of z and we obtain

2.2.5
$$\frac{\partial^2 \phi}{\partial x^2} + \frac{\partial^2 \phi}{\partial y^2} = \frac{qn_i}{\varepsilon_s} (e^{\beta(\phi-\phi_n-V_{BS})} - e^{-\beta(\phi-\phi_F-V_{BS})} + e^{\beta\phi_F} - e^{-\beta\phi_F}) \quad .$$

We now assume that the horizontal component of the electric field changes much more slowly than its vertical component, which implies

2.2.6
$$\frac{\partial^2 \phi}{\partial x^2} \gg \frac{\partial^2 \phi}{\partial y^2}$$

at any point of the channel. This assumption (called the gradual channel approximation) enables us to write

2.2.7
$$\frac{d^2 \phi}{dx^2} = \frac{qn_i}{\varepsilon_s} (e^{\beta(\phi-\phi_n-V_{BS})} - e^{-\beta(\phi-\phi_F-V_{BS})} + e^{\beta\phi_F} - e^{-\beta\phi_F}) \quad .$$

This can be integrated simply by noting that $\frac{d}{dx}\left(\left(\frac{d\phi}{dx}\right)^2\right) = 2\frac{d\phi}{dx}\frac{d^2\phi}{dx^2}$. Thus

$$\frac{d}{dx}\left(\left(\frac{d\phi}{dx}\right)^2\right) = \frac{2qn_i}{\beta\varepsilon_s}\left(e^{\beta(\phi-\phi_n-V_{BS})} - e^{\beta(-\phi+\phi_F+V_{BS})} + e^{\beta\phi_F} - e^{-\beta\phi_F}\right)\frac{d\phi}{dx} \quad ,$$

2.2.8
$$\left(\frac{d\phi}{dx}\right)^2_{x=\infty} - \left(\frac{d\phi}{dx}\right)^2_{x} = \frac{2qn_i}{\beta\varepsilon_s}\left\{\left[e^{\beta(\phi-\phi_n-V_{BS})} + e^{\beta(-\phi+\phi_F+V_{BS})} + \beta\phi\left(e^{\beta\phi_F} - e^{-\beta\phi_F}\right)\right]_{x=\infty}\right.$$

$$\left. - \left[e^{\beta(\phi-\phi_n-V_{BS})} + e^{\beta(-\phi+\phi_F+V_{BS})} + \beta\phi\left(e^{\beta\phi_F} - e^{-\beta\phi_F}\right)\right]_{x}\right\} \quad .$$

Our boundary conditions are that $\phi \to V_{BS}$ and $d\phi/dx \to 0$ as $x \to \infty$.

Simplifying we arrive at

2.2.9 $\quad \dfrac{d\phi}{dx}\bigg|_x = -\left(\dfrac{2qn_i}{\beta\varepsilon_s}\right)^{\frac{1}{2}}\left(e^{\beta(\phi-\phi_n-V_{BS})}+e^{\beta(-\phi+\phi_F+V_{BS})}+\beta(\phi-V_{BS})e^{\beta\phi_F}-e^{-\beta\phi_F})-e^{\beta\phi_F}-e^{-\beta\phi_n}\right)^{\frac{1}{2}}$

$\qquad\qquad = -\left(\dfrac{2qn_i}{\beta\varepsilon_s}\right)^{\frac{1}{2}} F(\phi,\phi_n)$,

where the dependence on ϕ_F and V_{BS} is implicit. Also, physical considerations necessitate taking the negative square root as can be seen by the location of $d\phi/dx$ in Figure (2.2.1). At the surface $x = 0$ and $\phi = \phi_s$. Therefore the electric field at the surface is a function of ϕ_s. Thus $\dfrac{d\phi}{dx}\bigg|_{x=0} = -\left(\dfrac{2qn_i}{\beta\varepsilon_s}\right)^{\frac{1}{2}} F(\phi_s,\phi_n)$. It is now possible to establish an implicit relation for the surface potential ϕ_s. Gauss' Law equates the change in electric displacement in a region to the charge enclosed in that region: $\int \varepsilon\, \vec{E} \cdot \vec{n}\, dA = \Sigma\, q_i$. However, we assume there to be no charge present in the oxide layer so the field will be constant from gate to surface. The electric displacement of the oxide layer, D_{ox}, can be calculated rather simply and equated with the electric displacement of the body, $\vec{D}_{body}$. Referring to Figure (2.2.1) we see that (for x-components)

$$E_{ox} = \dfrac{V_{GS}-\phi_s}{-t_{ox}} \qquad \text{and} \qquad E_{body} = -\left(\dfrac{2qn_i}{\beta\varepsilon_s}\right)^{\frac{1}{2}} F(\phi_s,\phi_n) \quad .$$

Therefore we may equate the two displacements

$$D_{ox} = -\dfrac{\varepsilon_{ox}}{t_{ox}}(V_{GS}-\phi_s) = -\alpha\, C_{ox}\, F(\phi_s,\phi_n) = D_{body}$$

where we have taken $C_{ox} = \dfrac{\varepsilon_{ox}}{t_{ox}}$ and $\alpha = \dfrac{1}{C_{ox}}\left(\dfrac{2qn_i\varepsilon_s}{\beta}\right)^{\frac{1}{2}}$.
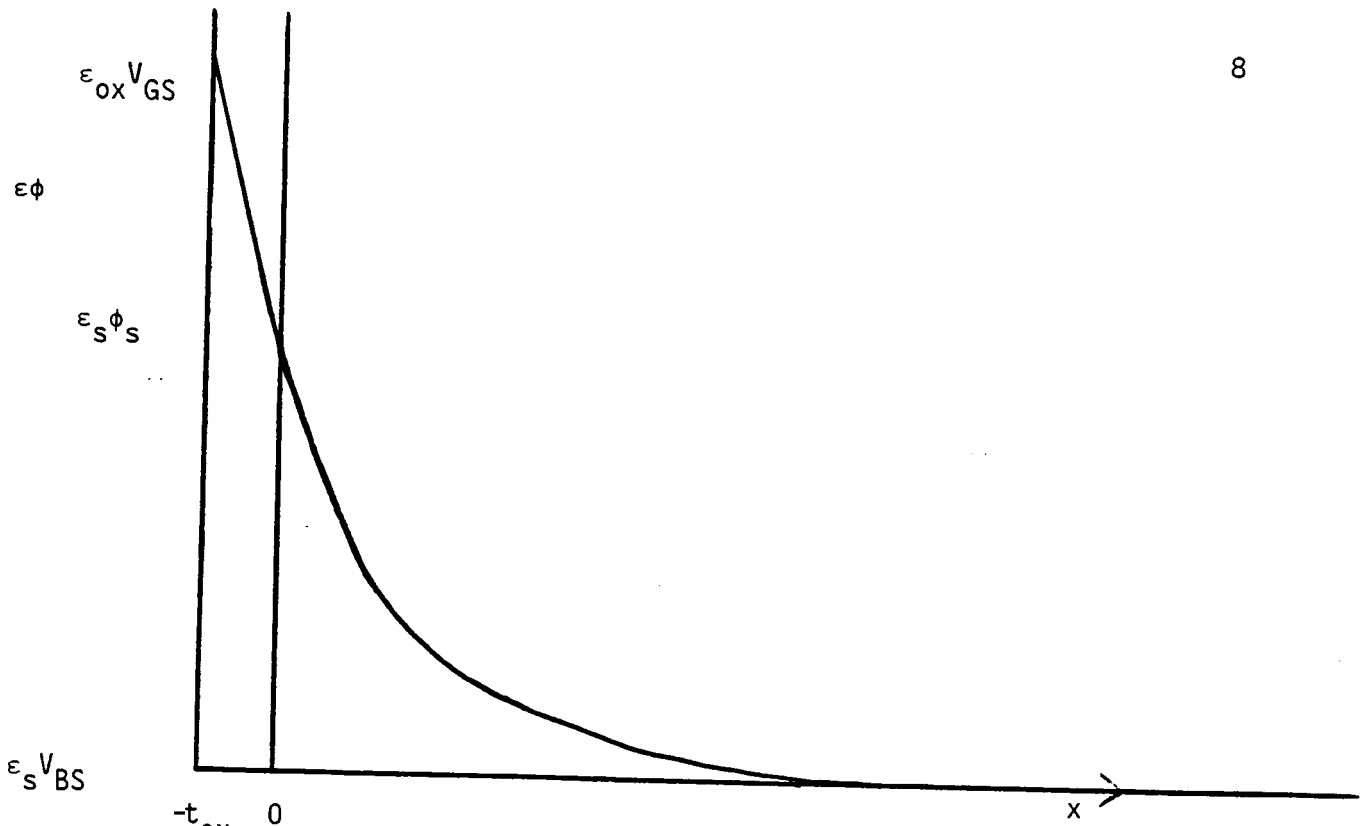
FIGURE 2.2.1

Top shows the graph of $\varepsilon\phi$ against x; the figure below shows a MOSFET side-on using the same x,y axes.

Finally ϕ_s is defined by the implicit expression

2.2.10 $\qquad \phi_s = V_{GS} - \alpha\, F(\phi_s, \phi_n)$

where

2.2.11 $\qquad F(\phi_s, \phi_n) = \left[e^{\beta(\phi_s - \phi_n - V_{BS})} + e^{\beta(-\phi_s + \phi_F + V_{BS})} \right.$

$$\left. + \beta(\phi_s - V_{BS})(e^{\beta\phi_F} - e^{-\beta\phi_F}) - e^{\beta\phi_F} - e^{-\beta\phi_n} \right]^{\frac{1}{2}} .$$

To obtain values for the source end of the channel we use the conditions:

$\phi_s = \phi_{S0}$ and $\phi_n = \phi_F - V_{BS}$. Similarly, for the drain end of the channel
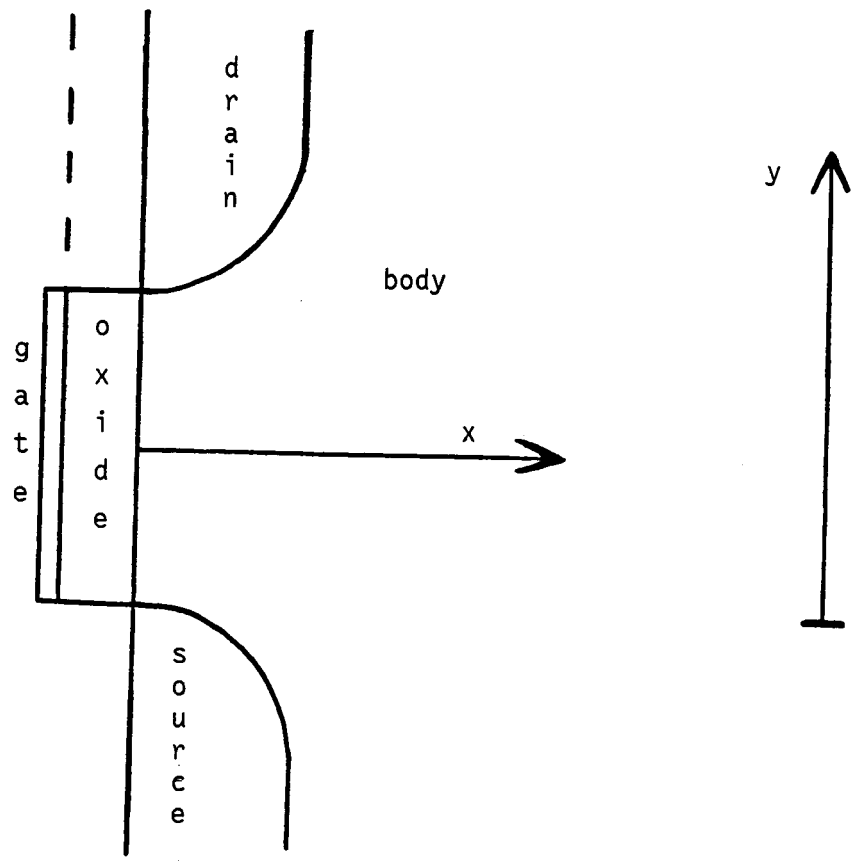
we use $\phi_s = \phi_{SL}$ and $\phi_n = \phi_F - V_{BS} + V_{DS}$. Equation (2.2.11) is the Pao-Sah

(see 2.4) exact one-dimensional expression for surface potential which can

be used to evaluate the potentials at the source and drain ends of the channel

by appropriate choice of ϕ_n.

The models of Brews and Van de Wiele presented in the next chapter use

different forms of (2.2.11) to obtain ϕ_{S0} and ϕ_{SL}. We shall now describe

their approach and we postpone to Chapter 5 a comparative numerical study

of the results obtained.

<u>Brews'computation of</u> ϕ_{S0} <u>and</u> ϕ_{SL}

In his derivation of surface potential Brews assumes the carrier densi-

ties (2.1.5a) and (2.1.5b). The surface potential expression itself is

derived by equating the space charge densities obtained through Gauss' Law

with the integral of a simplified Poisson's equation (see [3], pg. 19, see

also pg. 8). That is

2.2.12 $\qquad \rho = -C_{ox}(V_{GS}-\phi_s)$ $\qquad$ (Gauss) ,

2.2.13 $\qquad \rho = -C_{ox}\alpha\left[e^{\beta(\phi_s-\phi_n-V_{BS})}+\beta(\phi_s-V_{BS})e^{\beta\phi_F}-e^{-\beta\phi_n}\right]^{\frac{1}{2}}$ $\qquad$ (Poisson) .

Equating yields

2.2.14 $\qquad \phi_s = V_{GS} - \alpha\left[e^{\beta(\phi_s-\phi_n-V_{BS})}+\beta(\phi_s-V_{BS})e^{\beta\phi_F}\right]^{\frac{1}{2}}$.

Since at its largest value, $e^{-\beta\phi_n} < 10^{-5} \ll 1$, it has been neglected. Comparing (2.2.14) with (2.2.11) we see that while the expressions are obviously similar there are terms left out. These absent terms are a direct result of the way Brews takes Poisson's equation as $d^2\phi/dx^2 = q/\varepsilon_s\ (n+N_A)$, which considers only the effects of acceptor dopant ions and electrons (see [3], pg. 5). Accordingly, we find the terms associated with the donor dopant ions and the hole density to be missing in (2.2.13). This does not seem unreasonable considering their effect; near the surface, $(p+N_D)<(10^{-6}+10^{-6})\ll 1$, whereas $(n+N_A) > (10^6 + 10^6)$. Formula (2.2.14) is clearly just an approximation of the exact (2.2.11). It will be seen in Chapter 5 to be an excellent approximation "when appropriate".

Van de Wiele computation of ϕ_{S0} and ϕ_{SL}

The Van de Wiele model begins a little differently as the carrier densities are defined by the following:

2.2.16 $\qquad n = \dfrac{n_i^2}{N_A}\ e^{\beta(\phi-V(y))}$ $\qquad$ and $\qquad p = N_A e^{-\beta(\phi-V_{BS})}$.

With the relation $N_A = n_i e^{\beta \phi_F}$ we find

2.2.17 $\qquad n = n_i e^{\beta(\phi - V(y) - \phi_F)} \qquad$ and $\qquad p = n_i e^{\beta(-\phi + \phi_F + V_{BS})}$.

To Van de Wiele, $V(y) - V_{BS}$ accounts for the difference between the hole and electron quasi-Fermi levels ([11], pg. 991). In other words, $V(y) - V_{BS} = \phi_n - \phi_F$. Substituting this we find the distributions to correspond precisely to our previously derived ones ((2.1.5a) and (2.1.5b)). The general expression for surface potential is derived in the same manner as Pao-Sah and Brews, namely equating charge densities. According to Van de Wiele (see [11], (6) and (3)):

2.2.18 $\qquad \rho(y) = -C_{ox}(V_{GS} - \phi_s) \qquad$ (Gauss) ,

2.2.19 $\qquad \rho(y) = -\alpha \, C_{ox} \left(e^{\beta(\phi_s - \phi_n - V_{BS})} + e^{\beta(-\phi_s + \phi_F + V_{BS})} + \beta(\phi_s - V_{BS} - 1/\beta) e^{\beta \phi_F} - e^{-\beta \phi_n} \right)^{\frac{1}{2}}$

$\qquad\qquad\qquad\qquad\qquad\qquad\qquad\qquad\qquad\qquad\qquad\qquad\qquad$ (Poisson).

Equating these yields his expression for surface potential:

2.2.20 $\qquad \phi_s = V_{GS} - \alpha \left(e^{\beta(\phi_s - \phi_n - V_{BS})} + e^{\beta(-\phi_s + \phi_F + V_{BS})} + \beta(\phi_s - V_{BS} - 1/\beta) e^{\beta \phi_F} - e^{-\beta \phi_n} \right)^{\frac{1}{2}}$.

We see that (2.2.20) differs from (2.2.11) only in the exclusion of the $e^{-\beta \phi_F}$ term. The fact that $e^{-\beta \phi_F} < 10^{-5} \ll 1$ makes this reasonable and accounts for the discrepancy. Comparing (2.2.20) to (2.2.14) we see the Van de Wiele model produces a closer mathematical correspondence to the exact solution (2.2.11) than the Brews model. However, for the purposes of approximate

calculations, Van de Wiele suggests distinguishing between strong and weak inversion of the surface (see [11], pg. 993). Strong surface inversion is associated with the joint condition $V_{GS} \gg V_T$ and $\phi_n - \phi_F + V_{BS} < V_1$, where V_1 is the potential at which the transition between inversion and depletion regimes occurs (this can be considered a drain saturation potential); and V_T, the threshold potential, is the particular gate potential for which V_1 becomes equal to the source potential (this is the minimum gate potential to produce an inversion regime). For this case, charge density is approximated by:

$$2.2.21 \qquad \rho = -\alpha \, C_{ox} \left(e^{\beta(\phi_s - \phi_n - V_{BS})} \right)^{\frac{1}{2}} \qquad \text{(Poisson)} \ .$$

Equating this with the expression from Gauss, (2.2.18), gives an implicit relation for surface potential in a strongly inverted device:

$$2.2.22 \qquad \phi_{ss} = V_{GS} - \alpha \left(e^{\beta(\phi_s - \phi_n - V_{BS})} \right)^{\frac{1}{2}} \ .$$

Weak inversion occurs when $V_{GS} \ll V_T$ or when $V_{GS} \gg V_T$ and $\phi_n - \phi_F + V_{BS} > V_1$.

In this case charge density is approximated by

$$2.2.23 \qquad \rho = -\alpha \, C_{ox} \left(\beta(\phi_s - V_{Bs} - \tfrac{1}{\beta}) e^{\beta\phi_F} \right)^{\frac{1}{2}} \qquad \text{(Poisson)} \ .$$

Equating this with (2.2.18) gives an implicit relation for surface potential in a weakly inverted device

$$2.2.24 \qquad \phi_{sw} = V_{GS} - \alpha \left(\beta(\phi_{sw} - V_{BS} - \tfrac{1}{\beta}) e^{\beta\phi_F} \right)^{\frac{1}{2}} \ .$$

Comparing (2.2.22) and (2.2.24) with (2.2.20) we notice missing terms.

Neglecting $e^{\beta(-\phi_s+\phi_F+V_{BS})}-e^{-\beta\phi_n}$ in (2.2.17) seems quite reasonable since they are $< 10^{-5} << 1$. To understand how (2.2.22) and (2.2.24) are derived we must consider the charge densities. The total space charge density is the sum of the free carrier and depletion charge densities, i.e., $\rho_{sc} = \rho_N + \rho_D$. ρ_N can be considered the effect due to electrons and ρ_D the effect due to holes and doping. We are now approximating the total space charge by

2.2.25
$$\rho_{sc} = -\alpha \, C_{ox}(e^{\beta(\phi_s-\phi_n-V_{BS})}+\beta(\phi_s-V_{BS} - \frac{1}{\beta})e^{\beta\phi_F})^{\frac{1}{2}} = \rho_N + \rho_D \ .$$

In a weakly inverted device we neglect the effect of free carriers which causes the first exponential to drop out, hence (2.2.23) and (2.2.24). In a strongly inverted device we assume the free carriers to be much greater than the holes and so the second exponential drops out, thus (2.2.21) and (2.2.22).

In the Brews model, one formula, (2.2.14), suffices for calculation of surface potential. In the Van de Wiele model one must first determine whether the surface is strongly or weakly inverted to choose the appropriate expression. Formulae (2.2.22) and (2.2.24) are clearly approximations of (2.2.11) but their accuracy will be seen to be poor relative to Brews.

To determine the surface potential at the two ends of the channel we must consider the change in the quasi-Fermi level, ϕ_n, based on its position. It is assumed that ϕ_n at the source end of channel and at the source itself are equal (see [3], pg. 20). Thus to calculate surface potential at the source end of the channel we may replace ϕ_n by $\phi_F - V_{BS}$ ([3], (4.22)). Similarly, ϕ_n at the drain end equals ϕ_n at the drain itself and we may replace

ϕ_n by $\phi_F - V_{BS} + V_{DS}$ ([3], (4.24)). These substitutions may be made in all three models. To sum up then, the three models generate four similar expressions for surface potential at the source and drain ends of the channel.

At the source end $(\phi_n = \phi_F - V_{BS})$:

Pao-Sah

2.2.26
$$\phi_{S0} = V_{GS} - \alpha\left(e^{\beta(\phi_{S0}-\phi_F)} + e^{\beta(-\phi_{S0}+\phi_F+V_{BS})} + \beta(\phi_{S0}-V_{BS})(e^{\beta\phi_F} - e^{-\beta\phi_F})\right.$$
$$\left. - e^{\beta\phi_F} - e^{-\beta(\phi_F-V_{BS}+V_{DS})}\right)^{\frac{1}{2}} \; ;$$

Brews

2.2.27
$$\phi_{S0} = V_{GS} - \alpha\left(e^{\beta(\phi_{S0}-\phi_F)} + \beta(\phi_{S0}-V_{BS})e^{\beta\phi_F}\right)^{\frac{1}{2}} \; ;$$

Van de Wiele

$$\phi_{SW0} = V_{GS} - \alpha\left(\beta(\phi_{SW0} - V_{BS} - \frac{1}{\beta})e^{\beta\phi_F}\right)^{\frac{1}{2}} \; ,$$

2.2.28

$$\phi_{SS0} = V_{GS} - \alpha\left(e^{\beta(\phi_{SS0}-\phi_F)}\right)^{\frac{1}{2}} \; .$$

At the drain end $(\phi_n = \phi_F - V_{BS} + V_{DS})$:

Pao-Sah

2.2.29
$$\phi_{SL} = V_{GS} - \alpha\left(e^{\beta(\phi_{SL}-\phi_F-V_{DS})} + e^{\beta(-\phi_{SL}+\phi_F+V_{BS})} + \beta(\phi_{SL}-V_{BS})\right.$$
$$\left. (e^{\beta\phi_F} - e^{-\beta\phi_F}) - e^{\beta\phi_F} - e^{-\beta(\phi_F-V_{BS}+V_{DS})}\right)^{\frac{1}{2}} \; ;$$

Brews

2.2.30
$$\phi_{SL} = V_{GS} - \alpha \left[e^{\beta(\phi_{SL} - \phi_F - V_{DS})} + \beta(\phi_{SL} - V_{BS}) e^{\beta\phi_F} \right]^{\frac{1}{2}} \quad ;$$

Van de Wile

$$\phi_{SWL} = V_{GS} - \alpha \left[\beta(\phi_{SWL} - V_{BS} - \frac{1}{\beta}) e^{\beta\phi_F} \right]^{\frac{1}{2}} \quad ,$$

2.2.31

$$\phi_{SSL} = V_{GS} - \alpha \left[e^{\beta(\phi_{SSL} - \phi_F - V_{DS})} \right]^{\frac{1}{2}} \quad .$$

2.3 Derivation of $J_n(x,y)$

The current in a MOSFET is the result of electron flow in the inversion layer, which is governed by the drain-to-source potential. This causes a drift towards the drain and a statistical diffusion due to heat energy. These two effects are summed up as follows:

2.3.1
$$I = \int (j_{drift} + j_{diff.}) dx \quad ,$$

2.3.2
$$j_{drift} = \mu Q_n \frac{\partial \phi}{\partial y} \quad ,$$

2.3.3
$$j_{diff.} = -qD \frac{\partial n}{\partial y} \quad ,$$

where D is the diffusion rate determined by the Einstein relation as

2.3.4
$$D = \frac{\mu}{\beta} \quad .$$

The current density due to drift is proportional to the product of mobility of electrons, number of electrons, and electric field along the channel.

Because no current leakage is assumed through the oxide and depletion layer except for negligible recombination effects, one may assume that the contribution of the vertical field component to the current is negligible with respect to the contribution of the longitudinal component.

The current density due to diffusion is proportional to the electron concentration gradient $\partial n/\partial y$ where the number n of electrons is determined by the potential ϕ, according to the Maxwell-Boltzman approximation to the Fermi-Dirac distribution. Here we allow

$$2.3.5 \qquad -qD \frac{\partial n}{\partial y} = -qD \frac{\partial}{\partial y} (n_i e^{\beta(\phi-V_{BS}-\phi_n)}) \quad .$$

Hence

$$2.3.6 \qquad j_{diff.} = -qD(\frac{\partial \phi}{\partial y} - \frac{\partial \phi_n}{\partial y}) \quad .$$

Equation (2.3.6) provides a much needed relation between the drift and diffusion components since both are now expressed in terms of the surface potential, ϕ, and the electron quasi-Fermi level ϕ_n. Note that the variation in concentration along the channel is accounted for by variations in surface potential, ϕ_s, and quasi-Fermi level, such that the electron distribution changes as one approaches the drain. Upon substitution of (2.3.6) and (2.3.2) into (2.3.1) we obtain

$$2.3.7 \qquad I = W\int q\mu n \frac{\partial \phi_n}{\partial y} dx$$

where the integral is over the inversion layer.

Knowing the electron concentration, n, and the quasi-Fermi level gradient $\partial\phi_n/\partial y$ at any cross-section of the channel we can derive the current flow through the section by integrating (2.3.7). The principle of conservation of charge will then allow us to eliminate the y-variable with an integration along the channel to obtain

2.3.8
$$I = \frac{W}{L} \iint q\mu n \, \frac{\partial\phi_n}{\partial y} \, dxdy \quad .$$

It is worthwhile to note that since the total current flow at any cross-section of the channel is the same, the diffusion portion of the current increases as the drift component diminishes and vice versa. The use of quasi-Fermi level for the electrons carries this information, by assuming that ϕ_n changes with y, while the Fermi level ϕ_F remains fairly constant.

2.4 The Pao-Sah Formula

The Pao-Sah formula is an "exact" one-dimensional expression for the drain current based on (2.3.8). We call it "exact" in the sense that no other simplifications are introduced in addition to the gradual channel approximation.

It is based upon the idea that at any point along the channel the current, I, is equal to the integral of the current density over the inversion layer:

2.4.1
$$I(y) = W \int_0^{x_i(y)} J_n(x,y)dx \quad .$$

Using the expression for current density, (2.3.7), one gets

2.4.2
$$I(y) = Wq\mu \int_{x_i(y)}^0 n(x,y) \, \frac{d\phi_n(y)}{dy} \, dx \quad .$$

Since the quasi-Fermi potential for electrons is assumed to be independent of x, the y-dependence may be removed by integrating both sides of (2.4.2) along the channel. Hence

$$2.4.3a \qquad I = \frac{Wq\mu}{L} \int_0^L \frac{d\phi_n(y)}{dy} \int_{x_i(y)}^0 n(x,y)dx \, dy$$

$$2.4.3b \qquad = \frac{Wq}{L} \int_{\phi_F-V_{BS}}^{\phi_F-V_{BS}+V_D} \int_{x_i(y)}^0 n(x,y)dx \, d\phi_n \quad .$$

The limits of the first integral in (2.4.3b) are the value of ϕ_n at the source and drain ends of the channel, as postulated in (2.1.4).

The inner integral of (2.4.3) must now be put in terms of ϕ_n and ϕ. This integral represents the charge present in the inversion layer at an arbitrary point in the channel, which is known as a function of potential. Using the Poisson equation (2.2.7), we may integrate once, using the boundary conditions that $\phi - V_{BS}$ and $d\phi/dx$ are equal to 0 at $x = \infty$. This obtains the function in equation (2.2.11), or

$$2.4.4 \qquad \frac{d\phi}{dx} = \frac{-F(\phi,\phi_n,\phi_F)}{\beta L_D} \quad .$$

Using this fact, we may express the inner integral of (2.4.3) as

$$2.4.5 \qquad \int_{x_i(y)}^0 n(x,y)dx = \int_{\phi_F+V_{BS}}^{\phi_s} \frac{n(\phi,\phi_F,\phi_n)d\phi}{\left(\frac{d\phi}{dx}\right)}$$

$$= \beta L_D n_i \int_{\phi_F+V_{BS}}^{\phi_s} \frac{e^{\beta(\phi-\phi_n+\phi_F-V_{BS})}}{F(\phi,\phi_n,\phi_F)} \, d\phi$$

where (ϕ_F+V_{BS}) and ϕ_s represent the value of ϕ at the bottom and top of the inversion layer, respectively.

Combining (2.4.5) with (2.4.3), we obtain the double integral formula

2.4.6
$$I = \frac{\beta L_D W q \mu n_i}{L} \int_{\phi_F - V_{BS}}^{\phi_F - V_{BS} + V_D} \int_{\phi_F + V_{BS}}^{\phi_s} \frac{e^{\beta(\phi - \phi_F + V_{BS})}}{F(\phi, \phi_n, \phi_F)} \, d\phi \, d\phi_n \quad .$$

This formulation is general, and valid in all regions of operation.

III. SIMPLIFIED LONG CHANNEL MODELS

3.1 The Pierret-Shields Single Integral Formula

The Pao-Sah double integral formula given in (2.4.6) is:

$$(3.1.1) \quad I_D = \frac{W\mu_s}{\sqrt{2}L \cdot L_D} \int_{\Phi_n(0)}^{\Phi_n(L)} \int_{\Phi_F}^{\Phi_s} \frac{e^{\beta(\Phi-\Phi_n)}}{F(\Phi,\Phi_n,\Phi_F)} \, d\Phi \, d\Phi_n$$

where $\quad \Phi_n(0) = \Phi_F - V_{BS}$

and $\quad \Phi_n(L) = V_{DS} + \Phi_F - V_{BS}$

Note that in this section, Φ is measured from the substrate.

The Φ integral is essentially over the inversion layer. Since Φ is small in the depletion region outside of inversion, we can subtract the $\Phi = 0$ value of electron concentration and extend the integration through the whole depletion region. Thus (3.1.1) becomes

$$(3.1.2) \quad I_D = \frac{W\mu_s}{\sqrt{2}L \cdot L_D} \int_{\Phi_n(0)}^{\Phi_n(L)} \int_0^{\Phi_s} \frac{e^{\beta(\Phi-\Phi_n)} - e^{-\beta\Phi_n}}{F(\Phi,\Phi_n,\Phi_F)} \, d\Phi \, d\Phi_n \quad ,$$

with

$$(3.1.3) \quad F(\Phi,\Phi_n,\Phi_F) = \{e^{\beta(\Phi-\Phi_n)} + e^{\beta(\Phi_F-\Phi)} + \beta\Phi(e^{\beta\Phi_F}) - e^{-\beta\Phi_n} - e^{\beta\Phi_F}\}^{\frac{1}{2}} .$$

The key thing to realise now is that

$$(3.1.4) \quad \frac{\partial F}{\partial \Phi_n} = \frac{-\beta}{2F(\Phi,\Phi_n,\Phi_F)} (e^{\beta(\Phi-\Phi_n)} - e^{-\beta\Phi_n}) \quad .$$

Thus (3.1.2) will become an integral with respect to F instead of Φ_n.

$$(3.1.5) \qquad I_D = \frac{-\sqrt{2}W\mu_s}{\beta L.L_D} \int_{\Phi_n(0)}^{\Phi_n(L)} \int_0^{\Phi_s} \frac{\partial F}{\partial \Phi_n} \, d\Phi d\Phi_n.$$

At this stage, referring to Figure 3.1.1, we change the order of integration to give:

$$(3.1.6) \qquad \int_{\Phi_n(0)}^{\Phi_n(L)} \left\{ \int_0^{\Phi_s} \frac{\partial F}{\partial \Phi_n} \, d\Phi \right\} d\Phi_n = \int_0^{\Phi_{SO}} \left\{ \int_{\Phi_n(0)}^{\Phi_n(L)} \frac{\partial F}{\partial \Phi_n} \, d\Phi_n \right\} d\Phi$$

$$+ \int_{\Phi_{SO}}^{\Phi_{SL}} \left\{ \int_{\Phi_n^*}^{\Phi_n(L)} \frac{\partial F}{\partial \Phi_n} \, d\Phi_n \right\} d\Phi ,$$

where the curve in Figure 3.1.1 is given parametrically by:

$$\Phi_n = \Phi_n^*(y)$$

$$\Phi = \Phi_s(y) .$$

For a given $\Phi_s(y)$, $\Phi_n^*(y)$ is specified by the Pao-Sah gate voltage relation (2.2.10).
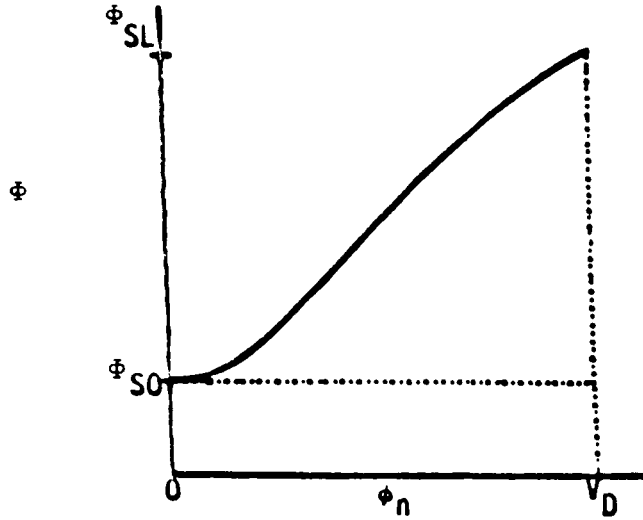
Figure 3.1.1 Curve $\Phi = \Phi_s(y)$, $\Phi_n = \Phi_n^*(y)$.

Hence we arrive at:

$$\int_{\Phi_n(0)}^{\Phi_n(L)} \int_0^{\Phi_s} \frac{\partial F}{\partial \Phi_n} d\Phi d\Phi_n = \int_0^{\Phi_{SL}} F(\Phi,V_D,\Phi_F)d\Phi - \int_0^{\Phi_{SO}} F(\Phi,0,\Phi_F)d\Phi$$

$$- \int_{\Phi_{SO}}^{\Phi_{SL}} F(\Phi_s,\Phi_n^*,\Phi_F)d\Phi_s \ .$$

We can evaluate the last term of (3.1.7) by referring to (2.2.10).

$$(V_{GB} - \Phi_s) \frac{\beta L_D C_{ox}}{\sqrt{2\mathcal{E}_s}} = F(\Phi_s,\Phi_n^*, \Phi_F) \ .$$

where $V_{GB} = V_{GS} - V_{BS}$.

The last integral thus becomes:

$$(3.1.9) \quad \int_{\Phi_{SO}}^{\Phi_{SL}} F(\Phi_s, \Phi_n^*, \Phi_F) d\Phi_s = \int_{\Phi_{SO}}^{\Phi_{SL}} (V_{GB} - \Phi_s) \frac{L_D C_{ox}}{\varepsilon_s} d\Phi_s$$

$$= \frac{\beta L_D C_{ox}}{\sqrt{2} \varepsilon_s} \left[V_{GB}(\Phi_{SL} - \Phi_{SO}) - \frac{1}{2}(\Phi_{SL}^2 - \Phi_{SO}^2) \right].$$

Thus we derived the single integral form of the Pao-Sah current expression:

$$(3.1.10) \quad I_D = \frac{W\mu C_{ox}\sqrt{2}}{\beta L} \left\{ V_{GB}(\Phi_{SL} - \Phi_{SO}) - \frac{1}{2}(\Phi_{SL}^2 - \Phi_{SO}^2) \right\}$$

$$+ \frac{W\mu \varepsilon_s \sqrt{2}}{\beta L \cdot L_D} \left\{ \int_0^{\Phi_{SO}} F(\Phi, \Phi_n(0), \Phi_F) d\Phi - \int_0^{\Phi_{SL}} F(\Phi, \Phi_n(L), \Phi_F) d\Phi \right\}$$

where Φ_{SO} and Φ_{SL} are calculated by

$$(3.1.11) \quad V_{GB} = \Phi_{SO} + \frac{\sqrt{2}\varepsilon_s}{\beta L_D C_{ox}} F(\Phi_{SO}, \Phi_n(0), \Phi_F), \text{ and}$$

$$(3.1.12) \quad V_{GB} = \Phi_{SL} + \frac{\sqrt{2}\varepsilon_s}{\beta L_D C_{ox}} F(\Phi_{SL}, \Phi_n(L), \Phi_F).$$

3.2 Brews Model

The Brews charge-sheet model is derived with the same reasoning which leads to the double integral form mentioned in (2.4). The number of electrons in the inversion layer is estimated using the charge-sheet approximation and the current density at any point of the channel is found to be

$$3.2.1 \qquad I = \mu Q_n \frac{\partial \phi_n}{\partial y}$$

where Q_n is the charge of electrons/unit area and ϕ_n is the quasi-Fermi level for electrons. We now illustrate the method used by Brews for computing Q_n and $\partial \phi_n / \partial y$.

To do these calculations we need to know how charge is assumed to be distributed within the device; this is virtually the defining characteristic of any simplified one-dimensional model.

The important thing to realize in Brews' derivation, is that he only considers two types of charge in the MOSFET; namely free electrons, n, and ionized acceptors, N_A.

The omission of ionized donor charge, N_D, is acceptable, since it always occurs with N_A in the form $N_A - N_D$. Since $N_D \ll N_A$, the approximation $N_A - N_D \cong N_A$ is seen to be good.

The omission of charge due to majority carriers (for n-channel devices these are holes, p) is more noteworthy. In fact, p is very small at the surface, and remains small up to some considerable depth--this is essentially the depletion region. Proceeding deeper into the device (x increasing) p tends asymptotically to N_A, its value in the bulk. Thus there is no definite lower boundary to the depletion region. The approximation Brews uses is that p = 0 down to some depth x = w, where it attains its asymp-

totic value. Thus we can think of the charge being distributed in the following manner. At the surface is an infinitely thin "charge sheet" of electrons; below this there is solely the constant doping charge, N_A, down to some depth w; beyond this, charge neutrality exists.

To find the current, we will first deal with Q_n. Since direct evaluation is very difficult Brews uses the equality

3.2.2 $$Q_n = Q_s - Q_D$$

where Q_s is the total charge/unit area and Q_D is the charge/unit area in the depletion layer due to ionized impurities. This is found to be

3.2.3 $$Q_D = -qN_Aw$$

with w equal to the depth of the depletion region. At this point we encounter one of the most questionable steps of Brews' derivation. To obtain w he writes

3.2.4 $$\frac{d^2\phi}{dx^2} = \frac{qN_A}{\varepsilon} \qquad 0 < x < w$$

which holds in the depletion region before inversion takes place. Therefore, using the conditions $\phi = V_{BS}$, $d\phi/dx = 0$ at $x = w$ we have

3.2.5 $$\phi(x) = V_{BS} + \frac{qN_A}{2\varepsilon_s}(x-w)^2$$

Now it is assumed that (3.2.5) remains true after inversion and can be extended to find ϕ_s, the value of ϕ at $x = 0$. This gives us

3.2.6 $$w = \sqrt{2}\, L_B(\beta\phi_s - \beta V_{BS})^{\frac{1}{2}} \quad .$$

Brews then states (but does not use) the result

3.2.7
$$w = \sqrt{2} \ L_B (\beta\phi_s - \beta V_{BS} - 1)^{\frac{1}{2}}$$

which he claims (without proof) comes from a "more accurate derivation that includes majority carriers more carefully".

(3.2.3) and (3.2.6) give us

3.2.8
$$Q_D = -\sqrt{2} \ q N_A L_B (\beta\phi_s - \beta V_{BS})^{\frac{1}{2}} \ .$$

To complete the expression for Q_n, we need to find Q_s. Continuity of the field across the oxide-silicon interface gives us the following:

3.2.9
$$\varepsilon_{ox} \left. \frac{d\phi}{dx} \right|_{x=0^-} = \varepsilon_s \left. \frac{d\phi}{dx} \right|_{x=0^+} \ .$$

The left-hand side of (3.2.9) is given by

3.2.10
$$\varepsilon_{ox} \left. \frac{d\phi}{dx} \right|_{x=0^-} = - \frac{\varepsilon_{ox}}{t_{ox}} (V_{GS} - \phi_s) = -C_{ox}(V_{GS} - \phi_s) \ .$$

Finally, Gauss' Law gives us Q_s to be

3.2.11
$$Q_s = \varepsilon_s \left. \frac{d\phi}{dx} \right|_{x=0^+} = -C_{ox}(V_{GS} - \phi_s) \ .$$

Thus we have

3.2.12
$$Q_n = \sqrt{2} \ q N_A L_B (\beta\phi_s - \beta V_{BS})^{\frac{1}{2}} - C_{ox}(V_{GS} - \phi_s) \ .$$

Now we turn to the calculation of $d\phi_n/dy$.

To find this, we relate ϕ_n to ϕ_s using once again the continuity of field at the surface (x = 0). The right-hand side of (3.2.9) is found by integrating the following initial value problem:

3.2.13
$$\frac{d^2\phi}{dx^2} = \begin{cases} \dfrac{qN_A}{\epsilon_s} + \dfrac{qn_i}{\epsilon_s}\, e^{\beta(\phi - V_{BS} - \phi_n)} & 0 \le x < w \\ \\ 0 & w < x \end{cases}$$

$\dfrac{d\phi}{dx} = 0$ and $\phi = V_{BS}$ at $x = w$.

Evaluation at the surface, $x = 0$, $\phi = \phi_s$ gives:

3.2.14
$$\left.\frac{d\phi}{dx}\right|_{x=0^+} = \frac{-\sqrt{2}}{\beta L_B}\left[\beta(\phi_s - V_{BS}) + \left(\frac{n_i}{N_A}\right)^2 e^{\beta(\phi_F - \phi_n)}\left(e^{\beta(\phi_s - V_{BS})} - 1\right)\right]^{\frac{1}{2}} .$$

With (3.2.4) and (3.2.10), (3.2.9) becomes

3.2.15
$$C_{ox}(V_{GS} - \phi_s) = \frac{\sqrt{2}\,\epsilon_s}{\beta L_B}\left[\beta(\phi_s - V_{BS}) + \left(\frac{n_i}{N_A}\right)^2 e^{\beta(\phi_F - \phi_n)}\left(e^{\beta(\phi_s - V_{BS})} - 1\right)\right]^{\frac{1}{2}}$$

which, after some manipulations gives

3.2.16
$$\beta\phi_n = \beta\phi_F - \ell n\, \frac{(\beta V_{GS} - \beta\phi_s)^2/a^2 - \beta(\phi_s - V_{BS})}{\left(\frac{n_i}{N_A}\right)^2 \left(e^{\beta(\phi_s - V_{BS})} - 1\right)}$$

with

3.2.17
$$a = \frac{\sqrt{2}\,\epsilon_s}{C_{ox} L_B} .$$

With $\partial\phi_n/\partial y$ obtained from (3.2.15) and Q_n given by (3.2.12) Brews writes (3.2.1) as

3.2.18
$$I = \frac{W\mu C_{ox}}{\beta}\left[\beta(V_{GS} - \phi_s) - a(\beta\phi_s - V_{BS})^{\frac{1}{2}} + \frac{2\beta(V_{GS} - \phi_s) + a^2}{\beta(V_{GS} - \phi_s) + a(\beta\phi_s - \beta V_{BS})^{\frac{1}{2}}}\right]\frac{d\phi_s}{dy}$$

Rather than integrate this exactly with respect to y, Brews notes that the second bracketed term (the fraction) will be important only when the first becomes negligible. Since the first represents Q_n, it will be small only near pinch-off. But, in this case we can write

3.2.19
$$\frac{2\beta(V_{GS}-\phi_s)+a^2}{\beta(V_{GS}-\phi_s)+a(\beta\phi_s-\beta V_{BS})^{\frac{1}{2}}} \cong 1 + \frac{a}{2(\beta\phi_s-\beta V_{BS})^{\frac{1}{2}}} \quad .$$

Then

3.2.20
$$I = \frac{W\mu C_{ox}}{\beta} \frac{d}{dy} \left\{ \left[\beta V_{GS} - \tfrac{1}{2}\beta\phi_s - \frac{2a}{3}(\beta\phi_s-\beta V_{BS})^{\frac{1}{2}} + 1 + a(\beta\phi_s-\beta V_{BS})^{-\frac{1}{2}} \right]\phi_s \right\} \quad .$$

Integrating (3.2.20) from 0 to L one obtains the source-to-drain current in terms of ϕ_{SO} and ϕ_{SL}, the potentials at the source and drain end of the channel as given by (2.2.27) and (2.2.30)

3.2.21
$$I = \frac{W\mu C_{ox}}{L\beta^2} \left[(1+\beta V_{GS})(\beta\phi_{SL}-\beta\phi_{SO}) - \tfrac{1}{2}[(\beta\phi_{SL})^2-(\beta\phi_{SO})^2] \right.$$

$$- \frac{2a}{3}[\beta\phi_{SL}-\beta V_{BS})^{3/2}-(\beta\phi_{SO}-\beta V_{BS})^{3/2}]$$

$$\left. + a[(\beta\phi_{SL}-\beta V_{BS})^{1/2}-(\beta\phi_{SO}-\beta V_{BS})^{1/2}] \right] \quad .$$

3.3 The Van de Wiele Model [11]

Van de Wiele uses a quasi-Fermi level formulation for carrier densities as in (2.1).

From (2.2) we see that his general surface potential equation is given by

3.3.1
$$\phi_s = V_{GS} - \left(\frac{2\varepsilon_s q n_i}{\beta}\right)^{\frac{1}{2}} F(\phi_s, \phi_n)$$

with

3.3.2
$$F(\phi_s, \phi_n) = \left\{ e^{\beta(\phi_s - V_{BS} - \phi_n)} + e^{\beta(\phi_F + V_{BS} - \phi_s)} + [\beta(\phi_s - V_{BS}) - 1]e^{\beta\phi_F} - e^{-\beta\phi_n} \right\}^{\frac{1}{2}} .$$

Differentiating (3.3.1) with respect to ϕ_s yields

3.3.3
$$\frac{d\phi_n}{d\phi_s} = 1 + \frac{e^{-\beta(\phi_n + \phi_F)} + 2\beta K(V_{GS} - \phi_s) + 1 - e^{\beta(V_{BS} - \phi_s)}}{\beta^2 K(V_{GS} - \phi_s)^2 + 1 + V_{BS} - \beta\phi_s - e^{\beta(V_{BS} - \phi_s)}}$$

where $K = \dfrac{C_{ox}^2}{2\beta q N_A \varepsilon_s}$.

Now, $\beta(\phi_s - V_{BS}) > \beta\phi_F > 11$ and $\beta\phi_F + \beta\phi_n \geq \beta\phi_F > 11$. Thus $e^{-\beta(\phi_n + \phi_F)} < 10^{-10}$ and $e^{\beta(V_{BS} - \phi_s)} < 10^{-5}$.

Hence the following is a good approximation to (3.3.3):

3.3.4
$$\frac{d\phi_n}{d\phi_s} = 1 + \frac{2\beta(V_{GS} - \phi_s) + M}{\beta^2(V_{GS} - \phi_s)^2 - M\beta(\phi_s - V_{BS} - 1)}$$

where $M = \dfrac{1}{K} = \dfrac{2\beta q N_A \varepsilon_s}{C_{ox}^2}$.

For the current, the same approach as (2.3) is taken, but with an effective mobility μ_{eff} introduced:

3.3.5
$$\int_0^L \frac{dy}{\mu n} = \frac{L}{\mu_{eff}} \quad .$$

Hence

3.3.6
$$I_D = - \frac{\mu_{eff} W}{L} \int_{\phi_n(0)}^{\phi_n(L)} Q_n \, d\phi_n$$

where $\phi_n(0) = \phi_F - V_{BS}$ and $\phi_n(L) = \phi_F + V_{DS} - V_{BS}$ as in (2.2).

Now we use

3.3.7
$$Q_n = Q_{SC} - Q_D$$

with

3.3.8
$$Q_{SC} = \varepsilon_s \times (\text{field at the surface}) = -C_{ox}(V_{GS} - \phi_s)$$

and

3.3.9
$$Q_D = - \left(\frac{2\varepsilon_s q N_A}{\beta} \right)^{\frac{1}{2}} (\beta(\phi_s - V_{Bs}) - 1)^{\frac{1}{2}} \quad .$$

(3.3.9) is equivalent to (3.2.8) in Brews' calculations.

Thus (3.3.6) becomes

3.3.10
$$I_D = \frac{\mu_{eff} W}{L} \int_{\phi_n(0)}^{\phi_n(L)} \left\{ C_{ox}(V_{GS} - \phi_s) - \left(\frac{2\varepsilon_s q N_A}{\beta} \right)^{\frac{1}{2}} (\beta(\phi_s - V_{BS}) - 1)^{\frac{1}{2}} \right\} d\phi_n \quad .$$

By using (3.3.4), we find that:

3.3.11
$$I_D = \frac{\mu_{eff}WC_{ox}}{L} \int_{\phi_{SO}}^{\phi_{SL}} \left\{ \beta(V_{GS}-\phi_s) - \sqrt{M}(\beta\phi_s - \beta V_{BS} - 1)^{\frac{1}{2}} \right\}$$

$$\left\{ 1 + \frac{2\beta(V_{GS}-\phi_s)+M}{\beta^2(V_{GS}-\phi_s)^2 - M(\beta(\phi_s-V_{BS})-1)} \right\} d\phi_s$$

i.e.:

3.3.12
$$\frac{\beta L I_D}{\mu_{eff}WC_{ox}} = \beta V_{GS}(\phi_{SL}-\phi_{SO}) - \frac{\beta}{2}(\phi_{SL}^2 - \phi_{SO}^2) - \frac{2}{3}\beta\sigma(A^{3/2}-B^{3/2})$$

$$+ \int_{\phi_{SO}}^{\phi_{SL}} \frac{2\beta(V_{GS}-\phi_s)+M}{\beta(V_{GS}-\phi_s)+\sqrt{M}(\beta\phi_s-\beta V_{BS}-1)^{\frac{1}{2}}} d\phi_s \quad .$$

A.M.E.T. (after much elementary tedium) we find:

3.3.13
$$I_D \frac{L}{W} \frac{\beta}{\mu_{eff}C_{ox}} = \left\{ (\beta V_{GS}-1)(\phi_{SL}-\phi_{SO}) - \frac{\beta}{2}(\phi_{SL}^2-\phi_{SO}^2) - \right.$$

$$\left. \frac{2}{3}\sigma\beta(A^{3/2}-B^{3/2})+\sigma(A^{1/2}-B^{1/2}) \right\} +$$

$$\left\{ (\phi_{SL}-\phi_{SO})+3\sigma(A^{1/2}-B^{1/2}) + \right.$$

$$\sigma^2 \ln \frac{\phi_{SL}-\sigma A^{\frac{1}{2}}-V_{GS}}{\phi_{SO}-\sigma B^{\frac{1}{2}}-V_{GS}} +$$

$$\left. 2\sigma C^{\frac{1}{2}} \ln \left[\frac{A^{\frac{1}{2}}-C^{\frac{1}{2}}-\frac{\sigma}{2}}{B^{\frac{1}{2}}-C^{\frac{1}{2}}-\frac{\sigma}{2}} \frac{B^{\frac{1}{2}}+C^{\frac{1}{2}}-\frac{\sigma}{2}}{A^{\frac{1}{2}}+C^{\frac{1}{2}}-\frac{\sigma}{2}} \right] \right\}$$

Where

$$A = \phi_{SL} - V_{BS} - \frac{1}{\beta}$$

$$B = \phi_{SO} - V_{BS} - \frac{1}{\beta}$$

$$C = V_{GS} - V_{BS} - \frac{1}{\beta} + \frac{\sigma^2}{4}$$

$$\sigma = \frac{(2\varepsilon_s q N_A)^{\frac{1}{2}}}{C_{ox}} \quad .$$

The part in the first parentheses is equivalent to (3.2.21) of Brews. Numerically, the second term in (3.3.13) is seen to be small compared to the first. If the approximation of [11], eqn. (3.2) is used in (3.3.11), it is seen that only the first term appears in the final current equation. Hence the Brews charge sheet result is an approximation of (3.3.13).

The derivation here of MOSFET current still depends crucially on the result $Q_D = -\sigma C_{ox}(\phi_s - V_{BS} - 1/\beta)^{\frac{1}{2}}$ as found in Brews (3.2.8). This is the step which we feel has not been sufficiently justified.

The surface potential schemes presented in (2.3) are seen to be inaccurate in some bias regimes. This is not a problem, however, since we can use the full one-dimensional equation to find ϕ_{SO} and ϕ_{SL} (see (2.3)).

Thus we conclude that, with the exception of using the result (3.3.9) for Q_D, the Van de Wiele derivation of drain current is based on assumptions and approximations which are nowhere too harsh. If the result (3.3.9) for Q_D were confirmed, then this model would be virtually optimal as a closed form of the one-dimensional Pao-Sah model.

3.4   The Clinic's Model

In the following section, we will give the details of a model derived by the Clinic which gives the drain current in all regimes of operation. It has not been possible to do a complete test on this model since the approach was devised very late in the semester. Some preliminary numerics do, however, indicate that this is certainly a valid model.

The strength of this model is in that, unlike previous models it does not use the same approximations over the whole range of operation of the device (a formidable task), or even, in fact over the whole device.

We have divided the device into regions A, B, and C . A full description of these regions is now given, together with various approximations valid therein.

REGION A

This is defined by

$$(3.4.1) \qquad \Phi_s > \Phi_n + V_{BS} + \Phi_F \; .$$

In this region, the surface is strongly inverted.

Let's look at the relative sizes of charge densities in the region.

$$(3.4.2) \qquad n = n_i \, e^{\beta(\Phi - V_{BS} - \Phi_n)}$$

$$(3.4.3) \qquad N_A = n_i \, e^{\beta \Phi_F}$$

$$(3.4.4) \qquad p = n_i \, e^{\beta(\Phi_F + V_{BS} - \Phi)}$$

Since we make comparisons with N_A , and $N_D \ll N_A$, we need not consider N_D .

Note that $\Phi_s > \Phi_F + V_{BS}$ and $e^{\beta \Phi_F} > 10^5$.

At the surface, $n > n_i e^{\beta\Phi_F}$, and thus $n/N_A > 1$. Also we have $p < n_i$ $e^{-\beta\Phi_n} < n_i e^{-\beta\Phi_F}$, and thus $p/N_A < 10^{-10}$! Hence $n/N_A - p \simeq n/N_A$.

Now consider a point at depth x_i beneath the surface where Φ falls to the value $V_{BS} + \Phi_n$. At this point $p/N_A = e^{-\beta\Phi_n}$ and $n/N_A = e^{-\beta\Phi_F}$; hence both are less than 10^{-5}. (Still we have $n/N_A - p \simeq n/N_A$.) This should now suggest the basis of the new approach.

Seeing how dramatically $n/N_A - p$ falls off between $x=0$ and x_i, we are justified in assuming that the contribution of charge due to electrons comes almost exclusively from the region $0 \leq x < x_i$.

The charge in the device below x_i is given by the field at x_i, namely

$$\varepsilon_s \frac{d\Phi}{dx}\bigg|_{x=x_i} = -\left[\frac{2qn_i s}{\beta}\right]^{\frac{1}{2}} F(\Phi_n + V_{BS}, \Phi_n) .$$

In the function F, the significant terms are:

$$e^{\beta(\Phi - V_{BS} - \Phi_n)} \; ; \; e^{\beta(\Phi_F + V_{BS} - \Phi)} \; ; \; (\beta\Phi - \beta V_{BS} - 1)e^{\beta\Phi_F} .$$

At $x = x_i$, we have that:

$$e^{\beta(\Phi - V_{BS} - \Phi_n)} = 1 \; ; \; e^{\beta(\Phi_F + V_{BS} - \Phi)} = e^{\beta(\Phi_F - \Phi_n)} \leq 1 \; ;$$

and

$$(\beta(\Phi - V_{BS}) - 1)e^{\beta\Phi_F} = (\beta\Phi_n - 1)e^{\beta\Phi_F} \geq (\beta\Phi_F - 1)e^{\beta\Phi_F} > 10^6 .$$

Thus at $x = x_i$

$$(3.4.5) \qquad F \simeq e^{\beta\Phi_F/2} \sqrt{\beta\Phi_n - 1}$$

In fact, neglecting the first term amounts to neglecting the contribution due to electrons.

Thus we have

(3.4.6) $\quad Q_D(A) \simeq -\left[\dfrac{2qN_A\varepsilon_s}{\beta}\right]^{\frac{1}{2}} \sqrt{\beta\phi_n - 1}$,

the charge beneath x_i due to N_A-p. We will refer to N_A-p as depletion charge.

Finally, we use the fact that the potential drops off rapidly as x increases from zero. This allows us to neglect the contribution of depletion charge from the region $0 \leq x < x_i$.

Hence Q_D is a good approximation for the total depletion charge in the device, and using Gauss' Law we find Q_n , the charge due to free electrons:

(3.4.7) $\quad Q_n(A) = Q_{sc} - Q_D(A)$

Now we use $Q_{sc} = \varepsilon_s \dfrac{d\phi}{dx}(x{=}0) = -C_{ox}(V_{GS}-\phi_s)$ to obtain

(3.4.8) $\quad Q_n(A) \simeq \left[\dfrac{2qN_A\varepsilon_s}{\beta}\right]^{\frac{1}{2}} \sqrt{\beta\phi_n - 1} - C_{ox}(V_{GS}-\phi_s)$.

We now make some definitions to be used throughout this chapter.

Definition 3.4.1

At any point along the channel, the region $o{\leq}x{<}x_i$ is defined to be the inversion layer.

Definition 3.4.2

At any point along the channel, $x = x_i$ is defined to be the depth at which $\phi = V_{BS} + \phi_n$.

Now let us move on to

Region B

(3.4.9) $\quad \phi_n < \phi_s - V_{BS} \leq \phi_n + \phi_F$

Once again, we approximate the depletion charge beneath x_i by (3.4.6).

Now, however, the inversion is not as strong. To account for the possibility of significant depletion charge in the inversion layer, we do the following calculation.

We still have $p/N_A = e^{-\beta(\Phi - V_{BS})} < e^{-\beta\Phi_F} < 10^{-5}$, hence if we can find x_i, then the depletion charge in the inversion layer is just $-qN_A x_i$.

$$(3.4.10) \qquad x_i = \int_0^{x_i} dx = \int_{\Phi_s}^{\Phi_n + V_{BS}} \frac{d\Phi}{\frac{d\Phi}{dx}} = \left[\frac{\beta\varepsilon_s}{2qn_i}\right]^{\frac{1}{2}} \int_{\Phi_s}^{\Phi_n + V_{BS}} \frac{d\Phi}{-F(\Phi, \Phi_n)}$$

$$(3.4.11) \qquad x_i = \left[\frac{\beta\varepsilon_s}{2qn_i}\right]^{\frac{1}{2}} \int_{\Phi_n + V_{BS}}^{\Phi_s} \frac{d\Phi}{F(\Phi, \Phi_n)} .$$

The significant terms of F are, once again:

$$(3.4.12) \qquad e^{\beta(\Phi - V_{BS} - \Phi_n)} ; \quad e^{\beta(\Phi_F + V_{BS} - \Phi)} ; \quad (\beta\Phi - \beta V_{BS} - 1) e^{\beta\Phi_F} .$$

For $\Phi_n + V_{BS} < \Phi \leq \Phi_s \leq \Phi_n + \Phi_F + V_{BS}$ we find that:

$$e^{\beta(\Phi-V_{BS}-\Phi_n)} < e^{\beta\Phi_F} \; ; \; e^{\beta(\Phi_F+V_{BS}-\Phi)} < 1 \; ; \; \text{and}$$

$$(\beta\Phi-\beta V_{BS}-1)e^{\beta\Phi_F} > (\beta\Phi_F-1)e^{\beta\Phi_F} > 11e^{\beta\Phi_F} \; .$$

If we retain only the third term, then we find that in the worst possible case $(\Phi_n = \Phi_F - V_{BS})$ <u>and</u> at the worst end of the integral, we have:

$$\frac{\frac{1}{F(approx.)} - \frac{1}{F(Correct)}}{\frac{1}{F(Correct)}} \simeq 0.04 \; .$$

Thus the approximation of keeping only term #3 is not at all too harsh. Hence the extra depletion charge is:

$$(3.4.13) \qquad -qN_A x_i \simeq -qN_A \left[\frac{\beta\epsilon_s}{2qN_A}\right]^{\frac{1}{2}} \int_{\Phi_n+V_{BS}}^{\Phi_s} (\beta\Phi-\beta V_{BS}-1)^{-\frac{1}{2}} d\Phi \; ,$$

$$(3.4.14) \qquad -N_A q x_i = -\Omega \left(\sqrt{\beta\Phi_s-\beta V_{BS}-1} - \sqrt{\beta\Phi_n-1} \right) \; ,$$

$$\text{where} \quad \Omega = \left[\frac{2qN_A\epsilon_s}{\beta}\right]^{\frac{1}{2}} \; .$$

Thus in region B, we approximate Q_n by:

$$(3.4.15) \qquad Q_n^{(B)} \simeq -C_{ox}(V_{GS}-\Phi_s) + \Omega\sqrt{\beta(\Phi_s-V_{BS})-1}$$

which is precisely the form used in Brews and Van der Wiele.

<u>NOTE:</u> We have derived this as a result of approximations which are only valid in region B . The approximation for x_i fails totally in region A.

Finally we look at

Region C

(3.4.16) $\Phi_S - V_{BS} < \Phi_n$

This is the pinch-off region. The potential has fallen below the effective Fermi-level, and thus the electron concentration is very small.

In this case, it is possible to evaluate Q_n directly.

$$(3.4.17) \qquad Q_n(C) = -q \int_0^{x^*} n(x,y)dy = -qn_i \left[\frac{\beta \epsilon_s}{2qn_i}\right]^{\frac{1}{2}} \int_{\Phi_F + V_{BS}}^{\Phi_S} \frac{e^{\beta(\Phi - V_{BS} - \Phi_n)}}{F(\Phi, \Phi_n)} d\Phi \quad .$$

The lower limit has been set to $\Phi_F + V_{BS}$ but this is subject to debate.

Referring to (3.4.12) we see that since $\Phi_F + V_{BS} < \Phi \leq \Phi_S < \Phi_n + V_{BS}$, the first and second terms of F are both less than one, whereas the third is at least 10^6. Thus we neglect all the terms of F except the third.

Then Q_n becomes

$$(3.4.18) \qquad Q_n(C) = \left[\frac{\beta q n_i \epsilon_s}{2e^{\beta \Phi_F}}\right]^{\frac{1}{2}} \int_{\Phi_F + V_{BS}}^{\Phi_S} \frac{e^{\beta(\Phi - V_{BS} - \Phi_n)}}{(\beta(\Phi - V_{BS}) - 1)^{\frac{1}{2}}} d\Phi \quad .$$

This approximation for F is still good if the lower limit of integration is extended to $\frac{1}{2}\Phi_F + V_{BS}$.

Under the substitution $t^2 = \beta(\Phi - V_{BS}) - 1$, this becomes:

$$(3.4.19) \qquad Q_n(C) = \left[\frac{2qn_i \varepsilon_s}{\beta e^{\beta \Phi_F}} \right]^{\frac{1}{2}} e^{1-\beta \Phi_n} \int_{(\beta \Phi_F - 1)^{\frac{1}{2}}}^{(\beta(\Phi_s - V_{BS}) - 1)^{\frac{1}{2}}} e^{t^2} dt \quad .$$

Since $-\Phi_n < V_{BS} - \Phi_s$, the equation for surface potential,

$$(3.4.20) \qquad V_{GS} - \Phi_s = K\{ e^{\beta(\Phi_s - V_{BS} - \Phi_n)} + e^{\beta(\Phi_F + V_{BS} - \Phi_s)}$$
$$+ (\beta \Phi_s - \beta V_{BS} - 1) e^{\beta \Phi_F} - e^{-\beta \Phi_n} \}^{\frac{1}{2}},$$

becomes essentially independent of Φ_n, and thus Φ_s will be constant in the whole pinched-off region, and the numerical integration in (3.4.19) need only be done once.

This concludes the discussion on Regions A, B, and C, in which we found simple expressions for Q_n. How do we find the current? Most generally, under a given set of applied voltages, parts of the device will be in each of the 3 regions A, B and C.

The current is given by

$$(3.4.21) \qquad I = - \frac{\mu W}{L} \int_{\Phi_n(0)}^{\Phi_n(L)} Q_n d\Phi_n$$

Since we have three different expressions for Q_n, it will be necessary to split the integral into three.

Consider a typical case where the source is in A, the drain in C, and a portion of the device in B.

The boundary between regions A and B is at $\Phi_n = \Phi_n^*$, $\Phi_s = \Phi_s^*$. This is defined to be the point along the channel where Φ_s becomes equal to $\Phi_n + \Phi_F + V_{BS}$ (by (3.4.9)).

Thus to find Φ_n^* we must solve the implicit equation (2.2.7) with $\Phi_s^* = \Phi_n^* + \Phi_F + V_{BS}$. Namely

$$(3.4.22) \qquad (V_{GS} - \Phi_n^* - \Phi_F - V_{BS}) = \left[\frac{2qn_i\epsilon_s}{\beta}\right]^{\frac{1}{2}} \frac{1}{C_{ox}} F(\Phi_n^* + \Phi_F + V_{BS}, \Phi_n^*) \ .$$

The boundary between regions B and C is defined to be where $\Phi_s = \Phi_n + V_{BS}$. When the drain is pinched off, the surface potential in the pinched-off region is constant and thus equal to Φ_{SL}. Hence this boundary is at $\Phi_n = \Phi_{SL} - V_{BS}$.

Thus the current is given by:

$$(3.4.23) \qquad I_D = -\frac{\mu W}{L}\left\{ \int_{\Phi_n(0)}^{\Phi_n^*} Q_n(A)d\Phi_n + \int_{\Phi_n^*}^{\Phi_{SL}-V_{BS}} Q_n(B)d\Phi_n + \int_{\Phi_{SL}-V_{BS}}^{\Phi_n(L)} Q_n(C)d\Phi_n \right\} \ .$$

Now we do the integrals.

$$(3.4.24) \qquad \int_{\Phi_n(0)}^{\Phi_n^*} Q_n(A)d\Phi_n = \int_{\Phi_n(0)}^{\Phi_n^*} [\Omega\sqrt{\beta\Phi-1} - C_{ox}(V_{GS}-\Phi_s)]\, d\Phi_n \qquad \text{or}$$

$$(3.4.25) \qquad \int_{\Phi_n(0)}^{\Phi_n^*} Q_n(A)d\Phi_n = \Omega(\sqrt{\beta\Phi_n^*-1} - \sqrt{\beta\Phi_n(0)-1}) - C_{ox}\int_{\Phi_{S0}}^{\Phi_s^*} (V_{GS}-\Phi_s)\frac{d\Phi_n}{d\Phi_s}\, d\Phi_s \ .$$

To evaluate the second term of (3.4.25), we use the approximation for $\dfrac{d\Phi_n}{d\Phi_s}$ used by Van der Wiele (3.3.4). The integral thus yields:

$$(3.4.26) \quad \int_{\Phi_n(0)}^{\Phi_n^*} Q_n(A)d\Phi_n = \Omega(\sqrt{\beta\Phi_n^*-1} - \sqrt{\beta\Phi_n(0)-1})$$

$$-\frac{C_{ox}}{\beta^2}\left\{ (\beta V_{GS}+2)(\beta\Phi_s^*-\beta\Phi_{S0}) + \frac{1}{2}\beta^2(\Phi_{S0}^2-\Phi_s^{*2}) \right.$$

$$+ \frac{M}{2}\ln\left[\frac{\beta^2(\Phi_s^*-V_{GS})^2 - M(\beta\Phi_s^* - \beta V_{BS}-1)}{\beta^2(\Phi_{S0}-V_{GS})^2 - M(\beta\Phi_{S0} - \beta V_{BS}-1)}\right]$$

$$\left. - a\ln\left[\frac{a+\beta\Phi_s^*-\beta V_{GS}-\frac{M}{2}}{a-\beta\Phi_s^*+\beta V_{GS}+\frac{M}{2}} \cdot \frac{a-\beta\Phi_{S0}+\beta V_{GS}+\frac{M}{2}}{a+\beta\Phi_{S0}-\beta V_{GS}-\frac{M}{2}}\right] \right\},$$

$$\text{where} \quad M = \frac{2\beta q N_A \varepsilon_s}{C_{ox}^2},$$

$$\text{and} \quad a = M(\frac{M}{4} + \beta V_{GS}-\beta V_{BS}-1).$$

The integral for region B is precisely that derived in Van der Wiele (3.3.13):

$$(3.4.27) \quad \int_{\Phi_n^*}^{\Phi_{SL}-V_{BS}} Q_n(B)d\Phi_n = \int_{\Phi_s^*}^{\Phi_{SL}} Q_n(B)\frac{d\Phi_n}{d\Phi_s}d\Phi_s$$

where

$$(3.4.28) \quad \int_{\Phi_n^*}^{\Phi_{SL}-V_{BS}} Q_n(B)d\Phi_n = -\frac{C_{ox}}{\beta} \left\{ (\beta V_{GS}-2)(\Phi_{SL}-\Phi_{SO}) - \frac{\beta}{2}(\Phi_{SL}^2-\Phi_{SO}^2) \right.$$

$$+ \frac{2}{3}\sigma\beta(A^{3/2} - B^{3/2}) + 4\sigma(A^{1/2} - B^{1/2})$$

$$+ \sigma^2 \ln\left[\frac{\Phi_{SL}-\sigma A^{1/2} - V_{GS}}{\Phi_{SO}-\sigma B^{1/2} - V_{GS}}\right]$$

$$\left. + 2\sigma C^{1/2} \ln\left|\frac{A^{1/2}-C^{1/2}-\frac{\sigma}{2}}{B^{1/2}-C^{1/2}-\frac{\sigma}{2}} \times \frac{B^{1/2}+C^{1/2}-\frac{\sigma}{2}}{A^{1/2}+C^{1/2}-\frac{\sigma}{2}}\right| \right\} ,$$

where

$$A = \Phi_{SL} - V_{BS} - \frac{1}{\beta}$$

$$B = \Phi_{SO} - V_{BS} - \frac{1}{\beta}$$

$$C = V_{GS} - V_{BS} - \frac{1}{\beta} + \frac{\sigma^2}{4}$$

$$\sigma = \frac{(2\epsilon_s q N_A)^{1/2}}{C_{ox}} .$$

Finally, the pinch-off contribution is given by:

$$(3.4.29) \quad \int_{\Phi_{SL}-V_{BS}}^{\Phi_n(L)} Q_n(C)d\Phi_n = \frac{e}{\beta}\left[\frac{2q n_i \epsilon_s}{\beta e^{\beta\Phi_F}}\right]^{1/2} \left[e^{\beta(V_{BS}-\Phi_{SL})}-e^{-\beta\Phi_n(L)}\right] \int_{(\beta\Phi_F-1)^{1/2}}^{(\beta(\Phi_{SL}-V_{BS})-1)^{1/2}} e^{t^2} dt$$

Thus (3.4.23) , along with (3.4.26, 28, 29) given the drain current when the source is in A and the drain pinched off (C).

If the drain is not pinched off, then the B integral goes all the way

to the drain, i.e. to $\Phi_n(L)$ or Φ_{SL} , and the C integral is omitted.

Similarly if the source is in region B, then the B integral starts at $\Phi_n(0)$ or Φ_{S0}, and the A integral is omitted.

Evidently this means that a single current expression is not obtainable by this approach. However, in each portion of the device, the equation giving the contribution of current is simple.

The contribution of current from region B of the device, is precisely that of Van der Wiele. It should be noted that the approximation we used to obtain this result breaks down when the device is strongly inverted (region A). It thus seems that a 'best' simple approximation in region A will not yield the Van der Wiele result. It is our belief that the treatment of region A in this report should turn out to be more accurate, but this MUST be tested numerically. A numerical testing of the various expressions for Q_n will have to be a very careful one, since in strong inversion the boundary layer at x=0 caused by the high electron concentration there will create problems for a general algorithm.

In conclusion, the strengths of this approach are that different approximations for Q_n are used through the device, depending on the level of inversion. The inclusion of a pinch-off term is also a much needed addition.

To fully complete this model, one of the following is required. Either a numerical testing which shows the value of Q_n to be accurate in region A, or a method of finding an integrable approximation for x_i , the inversion layer thickness.

IV. SOURCE AND DRAIN MODELLING

4.1. Purpose and Preliminaries

In the explicit formulae for drain current used by previous clinics for parameter extraction, the contribution of source and drain regions was limited to the inclusion of V_S (the potential at the source, usually grounded) and V_{DS} (the potential at the drain) in the derivation of Φ_{SO} and Φ_{SL}, the potentials at the source-end and drain-end of the channel respectively. Theoretical and experimental evidence suggest that this approximation is acceptable for long channel devices, but that it is one of the sources of disagreement between predicted and measured current in small devices, particularly when they are operated at low gate voltage ($V_{GS} \leq 2$) and negative substrate bias ($V_{BS} \leq -2$).

This year's clinic has contributed a more accurate analysis of source and drain regions and it has at least in part achieved the goal of incorporating in the drain current expression two quantities which were previously neglected:

- the source and drain doping profile;

- the ratio between the depth of the channel and the depth of the source and drain regions.

This result was achieved by applying variational techniques to determine the potential close to the ohmic contacts and methods of complex analysis to obtain the so called crowding resistance. We shall present here the source region analysis. The computations for the drain region are similar and are therefore omitted.
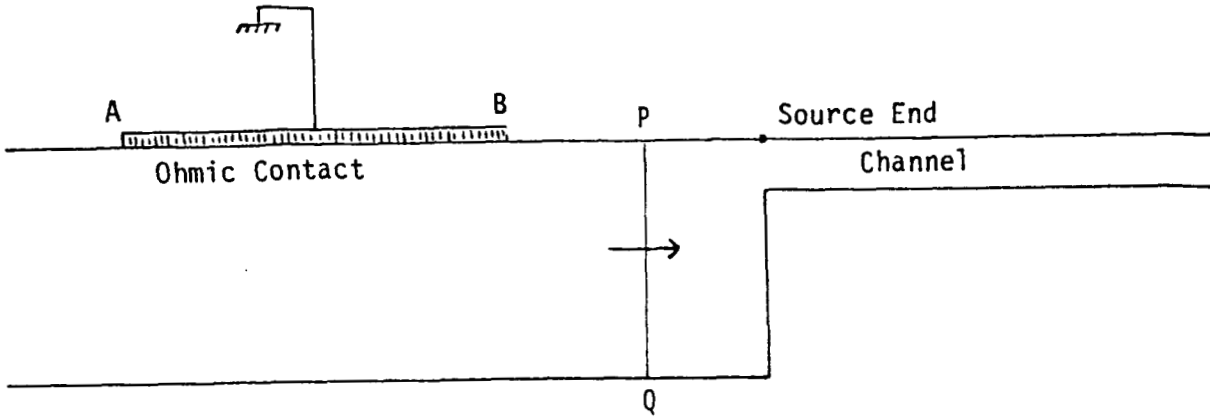
Figure 4.1.1

Figure 4.1.1 displays the two regions into which the source is divided. At the boundary PQ between the two regions the flow lines are assumed to be perpendicular to PQ. Region I is the ohmic contact area of the source and Region II is the crowding area. We shall present an analysis of Region I first.
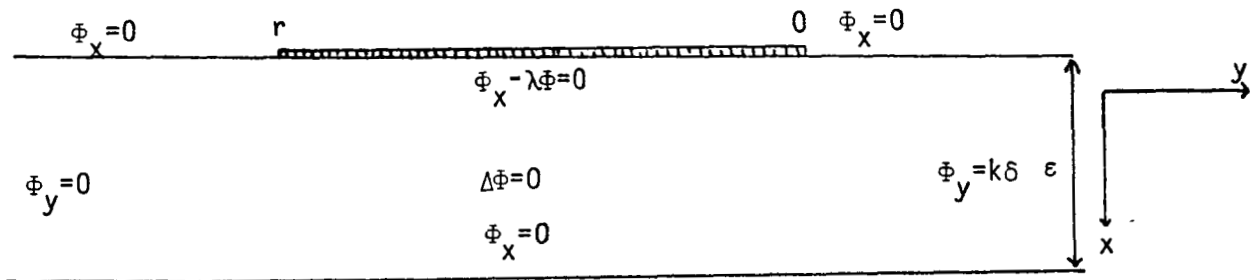
4.2. Ohmic Contact Region

Figure 4.2.1

Figure 4.2.1 shows the partial differential equation and the boundary conditions satisfied by the potential Φ in region I. We see that at the ohmic contact [-r;0] we have a Robin type boundary, while at the insulating boundaries the conditions are of Neumann type. The problem suggests that the potential Φ minimizes the functional

$$(4.2.1) \quad T(\Phi) = \int_{-\infty}^{+\infty} \int_{0}^{\varepsilon} \|\nabla\Phi\|^2 dxdy + \lambda \int_{-\infty}^{+\infty} \Phi^2(0,y)dy$$

with $\lambda = 0$ outside of $[-r, 0]$.

A first attempt at minimizing (4.3.1) can be tried by assuming that Φ is x-independent. We then obtain

$$(4.2.2) \quad \int_{-\infty}^{+\infty} (\varepsilon\Phi_y^2 + \lambda\Phi^2)dy = T(\Phi) \quad .$$

Therefore, using Euler's equation, we obtain

$$\varepsilon\Phi_{yy} - \lambda\Phi = 0$$

or

$$(4.2.3) \quad \begin{cases} \Phi = Me^{\sqrt{\frac{\lambda}{\varepsilon}}\,y} + Ne^{-\sqrt{\frac{\lambda}{\varepsilon}}\,y} & \text{in } (-r,0) \\ \Phi = ay + b & \text{in } (0, +\infty) \\ \Phi = cy + d & \text{in } (-\infty, 0) \end{cases}$$

The constants M,N,a,b,c,d, need be selected so that the boundary conditions and the continuity requirements are satisfied. We obtain

$$(4.2.4) \quad \Phi(y) = \begin{cases} A\cosh\left(\sqrt{\frac{\lambda}{\varepsilon}}\,y + B\right) & \text{in } (-r,0) \\ k\delta y + b & \text{in } (0, +\infty) \\ d & \text{in } (-\infty,0) \end{cases}$$

The four constants A, B, b, d satisfy the linear system.

(4.2.5)
$$\begin{cases} A \cosh B = b \\ \sqrt{\frac{\lambda}{\varepsilon}} \, A \sinh B = k\delta \\ A \cosh \left(- \sqrt{\frac{\lambda}{\varepsilon}} \, r + B\right) = d \\ \sqrt{\frac{\lambda}{\varepsilon}} \, A \sinh \left(-\sqrt{\frac{\lambda}{\varepsilon}} \, r + B\right) = 0 \end{cases}$$

Therefore

(4.2.6)
$$\begin{cases} B = \sqrt{\frac{\lambda}{\varepsilon}} \\ A = \dfrac{k\delta\sqrt{\frac{\varepsilon}{\lambda}}}{\sinh \sqrt{\frac{\lambda}{\varepsilon}} r} = d \\ b = k\delta \sqrt{\frac{\lambda}{\varepsilon}} \coth \sqrt{\frac{\lambda}{\varepsilon}} r \end{cases}$$

This approximation is obviously not optimal.

A better approximation to Φ can be obtained by assuming

(4.2.7)
$$\Phi(x,y) = m(y) + \frac{1}{\varepsilon^2} n(y)(x-\varepsilon)^2$$

Then m and n satisfy the systems of differential equations

(4.2.8)
$$\begin{cases} m" + \frac{1}{3} n" = \frac{\lambda}{\varepsilon} (m+n) \\ \frac{1}{3} m" + \frac{1}{5} n" = \frac{4}{3\varepsilon^2} n + \frac{\lambda}{\varepsilon} (m+n) \end{cases}$$

for $\quad \lambda \neq 0 \quad$ (in $(-r,0)$) , and

$$(4.2.9) \quad \begin{cases} m'' + \dfrac{1}{3}\, n'' = 0 \\[2mm] m'' + \dfrac{3}{5}\, n'' = \dfrac{4}{3\varepsilon^2}\, n \end{cases}$$

for $\quad \lambda = 0 \quad$ (outside $(-r,0)$). Setting

$$u = \sqrt{\dfrac{\lambda}{\varepsilon}}\, y \quad \text{and} \quad s = \sqrt{\dfrac{\lambda}{\varepsilon}}\, r$$

we obtain

$$(4.2.10) \quad \begin{cases} m_{uu} + \dfrac{1}{3}\, n_{uu} = m + n \\[2mm] \dfrac{1}{3}\, m_{uu} + \dfrac{1}{5}\, n_{uu} = \dfrac{4}{3\varepsilon\lambda}\, n + m + n \end{cases}$$

in $(-s, 0)$ and

$$(4.2.11) \quad \begin{cases} m_{uu} + \dfrac{1}{3}\, n_{uu} = 0 \\[2mm] m_{uu} + \dfrac{3}{5}\, n_{uu} = \dfrac{4}{\varepsilon\lambda}\, n \end{cases}$$

outside $(-s,0)$. Taking into account the boundary conditions on Φ_y we have

$$(4.2.12) \quad \begin{cases} m = -\dfrac{1}{3}\, B_2 e^{-\sqrt{\frac{15}{\varepsilon\lambda}}\, u} + k\delta\sqrt{\dfrac{\varepsilon}{\lambda}}\, u + B_3 \\[4mm] n = B_2 e^{-\sqrt{\frac{15}{\varepsilon\lambda}}\, u} \end{cases}$$

in $(0, +\infty)$, and

(4.2.13)

$$m = -\frac{1}{3} C_2 e^{\sqrt{\frac{15}{\lambda\varepsilon}}(u+\Gamma)} + C_3$$

$$n = C_2 e^{\sqrt{\frac{15}{\lambda\varepsilon}}(u+\Gamma)}$$

in $(-\infty, -s)$.

In $(-s, 0)$ the system (4.2.10) gives the following algebraic equation for n

(4.2.14) $\delta^4 - (6 + \frac{15}{\varepsilon\lambda}) \delta^2 + \frac{15}{\varepsilon\lambda} = 0$.

For $\lambda\varepsilon << 1$ we have

$$\delta_1 \simeq \sqrt{\frac{15}{\lambda\varepsilon} + 5} + \ldots \qquad\qquad \delta_2 \simeq -\sqrt{\frac{15}{\lambda\varepsilon} + 5} + \ldots$$

$$\delta_3 \simeq 1 \qquad\qquad\qquad\qquad \delta_4 \simeq -1 \qquad .$$

Accordingly $\qquad (\theta = \sqrt{\frac{15}{\varepsilon\lambda}})$

(4.2.15)

$$\begin{cases} n(u) \simeq A_1 e^{\theta u} + A_2 e^{-\theta u} + A_3 e^{u} + A_4 e^{-u} \\[2ex] m(u) \simeq -\frac{1}{3} A_1 e^{\theta u} - \frac{1}{3} A_2 e^{-\theta u} - \frac{2}{\varepsilon\lambda}(A_3 e^{u} + A_4 e^{-u}) \end{cases}$$

Continuity of m , m' , n , n' at $u = -s$ and $u = 0$ gives the following system of 8 linear equations in A_1, A_2, A_3, A_4, B_2, B_3, C_2, C_3.

$$\begin{cases} A_1 + A_2 + A_3 + A_4 = B_2 \\[1ex] \frac{1}{3}A_1 + \frac{1}{3}A_2 + \frac{2}{\varepsilon\lambda}A_3 + \frac{2}{\varepsilon\lambda}A_4 = \frac{1}{3}B_2 - B_3 \\[1ex] \theta(A_1-A_2) + A_3 - A_4 = -\theta B_2 \\[1ex] \frac{1}{3}\theta(A_1-A_2) + \frac{2}{\varepsilon\lambda}(A_3-A_4) = -\frac{1}{3}\theta B_2 - k\delta\sqrt{\frac{\varepsilon}{\lambda}} \end{cases} \qquad (u=0)$$

$$\begin{cases} A_1 e^{-\theta s} + A_2 e^{\theta s} + A_3 e^{-s} + A_4 e^{s} = C_2 \\[1ex] \frac{1}{3}A_1 e^{-\theta s} + \frac{1}{3}A_2 e^{\theta s} + \frac{2}{\varepsilon\lambda}A_3 e^{-s} + \frac{2}{\varepsilon\lambda}A_4 e^{s} = \frac{1}{3}C_2 - C_3 \\[1ex] \theta(A_1 e^{-\theta s} - A_2 e^{-\theta s}) + A_3 e^{-s} - A_4 e^{s} = \theta C_2 \\[1ex] \frac{1}{3}\theta(A_1 e^{-\theta s} - A_2 e^{\theta s}) + \frac{2}{\varepsilon\lambda}(A_3 e^{-s} - A_4 e^{s}) = \frac{1}{3}\theta C_2 \end{cases} \qquad (u=-s)$$

With $a = \frac{1}{3} - \frac{2}{\varepsilon\lambda}$ $\qquad b = k\delta\sqrt{\frac{\varepsilon}{\lambda}}$ $\qquad$ we find that

$$A_4 = \frac{b}{a(e^{2s}-1)} \qquad B_3 = aA_4(1+e^{2s})$$

$$A_3 = A_4 e^{2s} \qquad B_2 = A_1 + A_2 + A_3 + A_4$$

$$A_2 = -A_4 e^{s(1-\theta)} \qquad C_2 = A_1 e^{-\theta s} - A_2 e^{\theta s}$$

$$A_1 = A_4 \frac{(1-\theta)-e^{2s}(1+\theta)}{2\theta} \qquad C_3 = 2a A_4 e^{s}$$

Hence

$$A_1 \simeq + \frac{1}{4} k\delta\varepsilon\sqrt{\varepsilon\lambda}$$

$$A_2 \simeq \frac{1}{2} k\delta\varepsilon\sqrt{\varepsilon\lambda} \; e^{-s(1+\sqrt{\frac{15}{\varepsilon\lambda}})}$$

$$A_3 \simeq - \frac{1}{2} k\delta\varepsilon\sqrt{\varepsilon\lambda}$$

$$A_4 \simeq - \frac{1}{2} k\delta\varepsilon\sqrt{\varepsilon\lambda} \; e^{-2s}$$

$$B_2 \simeq - \frac{1}{4} k\delta\varepsilon\sqrt{\varepsilon\lambda}$$

$$B_3 \simeq k\delta\sqrt{\frac{\varepsilon}{\lambda}}$$

$$C_2 \simeq \frac{1}{2} k\delta\varepsilon\sqrt{\varepsilon\lambda}\left[\frac{1}{2} \; e^{-\sqrt{\frac{15}{\lambda\varepsilon}}s} + e^{-s}\right]$$

$$C_3 \simeq 2k\delta\sqrt{\frac{\varepsilon}{\lambda}} \; e^{-s} \quad .$$

Consequently

$$.2.16) \quad \Phi(x,y) \simeq \begin{cases} 0 & \text{if } y \le -r \\[2ex] \frac{1}{12} k\delta\sqrt{\frac{\lambda}{\varepsilon}} \left[e^{\sqrt{\frac{\lambda}{\varepsilon}}\,y} (12\frac{\varepsilon}{\lambda} - 6(x-\varepsilon)^2) + e^{\sqrt{15}\frac{y}{\varepsilon}}(3(x-\varepsilon)^2 - \varepsilon^2) \right] & \text{if } -r \le y \le 0 \\[2ex] \frac{k\delta}{12}\left[12\sqrt{\frac{\varepsilon}{\lambda}} + 12y + \varepsilon\sqrt{\varepsilon\lambda} \; e^{-\sqrt{15}\frac{y}{\varepsilon}} - 3\sqrt{\frac{\lambda}{\varepsilon}} \; e^{-\sqrt{15}\frac{y}{\varepsilon}}(x-\varepsilon)^2 \right] & \text{if } 0 \le y \; . \end{cases}$$

The neglected terms are exponentially small.

The current outflow is $(y = 0)$

$$(4.2.17) \quad \int_0^\varepsilon \Phi_y dx = k\delta\varepsilon$$

The current inflow is $(x = 0, \ y\varepsilon[-r,0])$

$$(4.2.18) \quad \int_{-r}^0 \Phi_x dy = k\delta\varepsilon - \frac{k\delta}{\sqrt{15}} \varepsilon\sqrt{\lambda\varepsilon} + \ldots$$

and we see that the two flows agree in first approximation.

The current inflow is concentrated in a boundary layer near $y = 0$. There are two layers, whose heights are $\sqrt{\varepsilon}$ and whose widths are $\sqrt{\varepsilon}$ and ε respectively (see figure 4.2.3). The solution is independent of r and the current enters (or leaves at the drain end) at the corner where the ohmic contact is closer to the channel. Hence we can assume that $r = \infty$. The current lines are represented in figure (4.2.4).

We can now compute the resistance between the equipotential line $(\Phi=0)$ AB (see figure 4.2.1) and the equipotential line PQ. Without going into the technical details (see [8]) of the calculations we shall simply mention that the resistance R_1 is given by

$$(4.2.19) \quad R_1^{-1} = \int_0^\varepsilon \left[\int |\nabla\Phi|^2 (\sigma_m \Phi_y)^{-1} dy + \rho_c (\nabla\Phi)_{x=0} \right]^{-1} dc$$

where σ_m is the silicon conductivity, ρ_c the contact resistivity, and where the inner integral is taken along each current line, $\psi = c$, from the region PQ to the contact. (ψ is the harmonic conjugate of the potential Φ.)

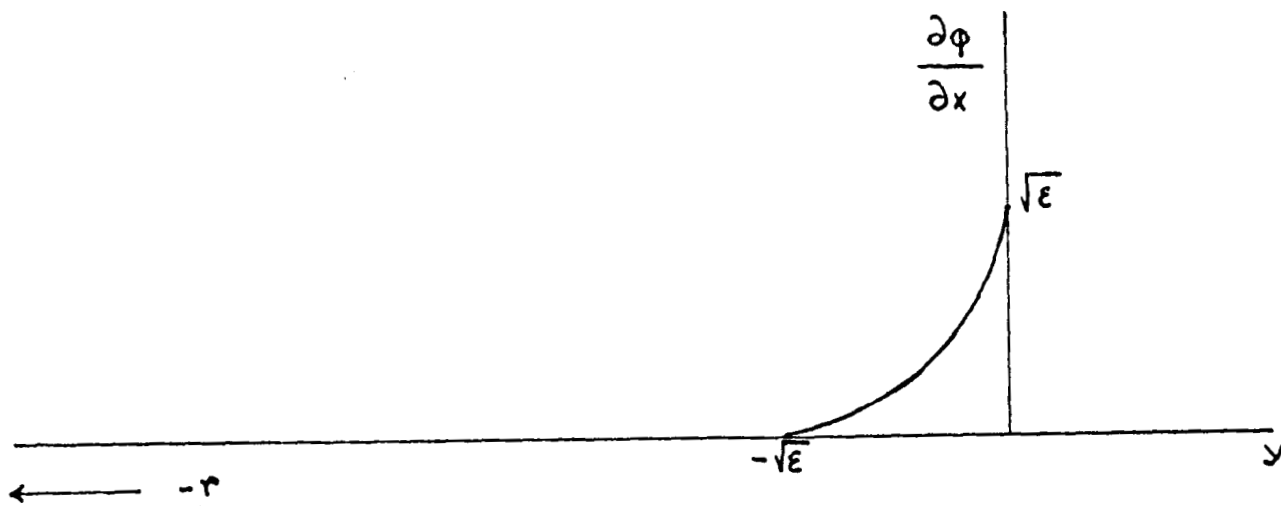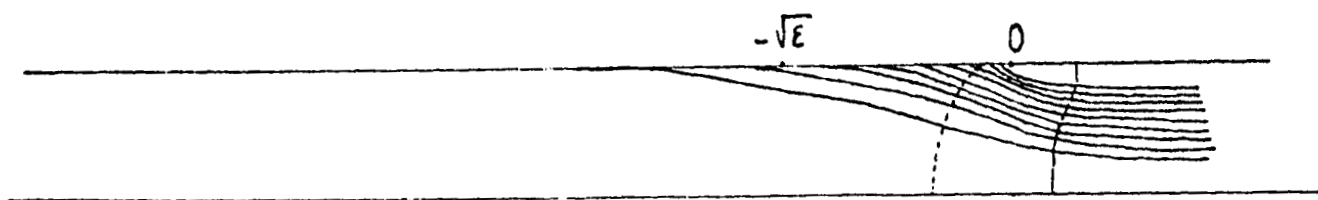We then have $\Phi(PQ) - \Phi(AB) = R_1 I$ and since $\Phi(AB) = 0$ we obtain

Figure 4.2.3

Figure 4.2.4

(4.2.20) $\Phi(PQ) = R_1 I$

4.3 The Crowding Resistance

As stated previously, this section will be concerned with the analysis of region II (see Figure 4.2.2) for the purpose of finding the crowding resistance, namely the resistance due to the distortion of the current lines near the junction where the source meets the channel of the device [9].

Here we will make use of the Schwarz-Christoffel transformation, [12]; a conformal mapping technique which maps the interior of a polygon in one plane into the upper half of a second plane bounded by the real axis and an infinite arc, or vice versa.
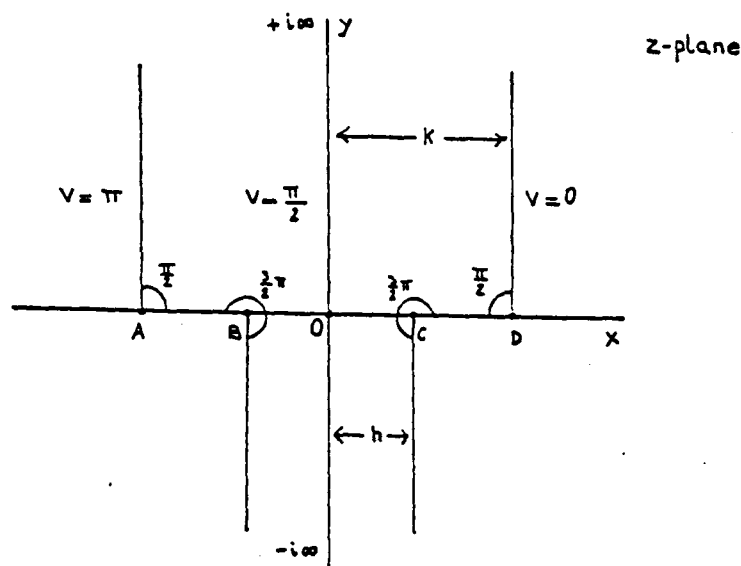
Figure 4.3.1

Figure 4.3.1 shows the geometry of the region we are interested in transforming with the Schwarz-Christoffel theorem; Figure 4.3.2, instead, contains the plane of the straight line into which the boundary of Figure 4.3.1 has been opened out:
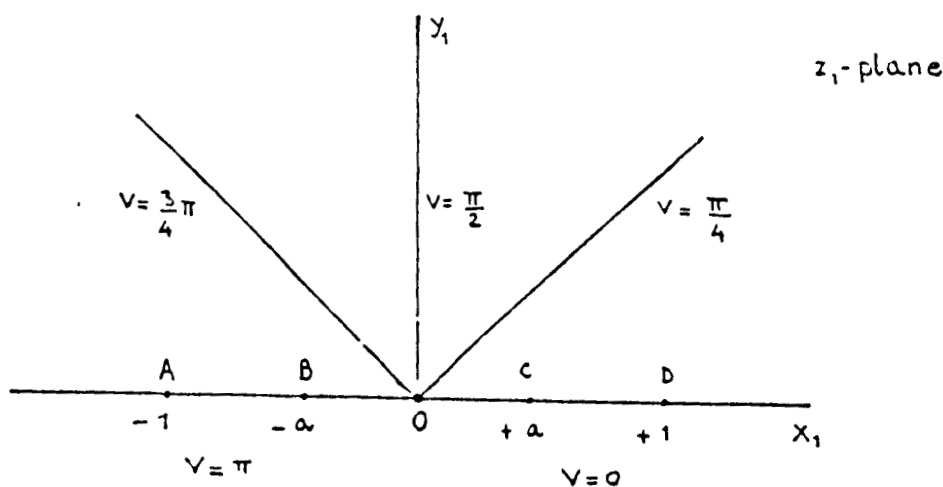
Figure 4.3.2

The differential equation:

$$(4.3.1) \quad \frac{dz}{dz_1} = c \frac{(z_1^2 - a^2)^{\frac{1}{2}}}{z_1(z_1^2-1)^{\frac{1}{2}}} = \frac{cz_1}{[(z_1^2-1)(z_1^2-a^2)]^{\frac{1}{2}}} - \frac{ca^2}{z_1[(z_1^2-1)(z_1^2-a^2)]^{\frac{1}{2}}}$$

is the expression given by Schwarz and Christoffel for the ratio between the two infinitesimal vectors dz and dz_1.

Letting $z_1 = Re^{i\alpha}$, the two constants c and a can be obtained through the evaluation of the following integral:

$$(4.3.2) \quad \int_{+h}^{-h} dz = ic \left[\int_0^\pi \left(\frac{R^2 e^{2i\alpha} - a^2}{R^2 e^{2i\alpha} - 1} \right)^{\frac{1}{2}} d\alpha \right]_{R \to 0} = \pm ic \int_0^\pi a\, d\alpha$$

and

$$(4.3.3) \quad \int_{+k}^{-k} dz = ic \left[\int_0^\pi \left(\frac{R^2 e^{2i\alpha} - a^2}{R^2 e^{2i\alpha} - 1} \right)^{\frac{1}{2}} d\alpha \right]_{R \to +\infty} = \pm ic \int_0^\pi d\alpha \; .$$

Substituting into (4.3.1) the expressions $a = \frac{h}{k}$ and $c = \frac{2k}{i\pi}$ obtained from (4.3.2) and (4.3.3) and integrating, we get:

$$(4.3.4) \quad z = \frac{2}{\pi} \left\{ k \tan^{-1}\left(\frac{z_1^2 - a^2}{1 - z_1^2}\right)^{\frac{1}{2}} + h \tan^{-1}\left(a\left(\frac{1 - z_1^2}{z_1^2 - a^2}\right)^{\frac{1}{2}} \right) \right\}$$

Set $W = U + iV$ (with U the potential and V the current flux vector) and $W = \ln z_1$ or $z_1 = e^W$; then clearly Figure 4.3.1 the current lines follow the right and left boundaries of the strip from top to bottom giving a total current $I = \frac{\pi}{s}$, s being the resistivity of the strip.

Substituting $z_1 = e^W$ and observing that the line of flow along the y - axis is $V = \frac{\pi}{2}$, we find:

$$(4.3.5) \quad y = \frac{\pi}{2} \left\{ k \tanh^{-1}\left[\frac{e^{2U} + a^2}{1 + e^{2U}}\right]^{\frac{1}{2}} - h \tanh^{-1}\left[a\left(\frac{1 + e^{2U}}{e^{2U} + a^2}\right)^{\frac{1}{2}} \right] \right\} .$$

By equating (4.3.5) to zero, we obtain that the potential V_0 at (x=0, y=0) must be approximately equal to λa when $a \ll 1$. The value $\lambda = 0.308705435$ has been computed for the parameter λ using Newton's method to solve the equation:

$$(4.3.6) \quad \tanh (\lambda^2 + 1)^{\frac{1}{2}} = \frac{1}{(\lambda^2 + 1)^{\frac{1}{2}}}$$

derived by equating (4.3.5) to zero with $U_0 = \ln \lambda a$.

The exact value for U_0 is obtained as an inverse function by setting

$$x = \left[\frac{e^{2U} + a^2}{e^{2U} + 1}\right]^{\frac{1}{2}}. \quad \text{Then} \quad U_0 = \frac{1}{2}\ln\left[\frac{x^2 + a^2}{1 - x^2}\right].$$

The substitution of x into (4.3.5) with y=0 plus a little algebra gives

the equation:

$$\frac{1-x}{1+x} = \left(\frac{x-a}{x+a}\right)^{\frac{1}{2}}$$

that we solved using Newton's method with values for a in the interval

(0.01,0.034).

Table 4.3.1 shows the numerical results computed for

(4.3.7) $U_0 = \ln \lambda a$ and

$$(4.3.8) \quad U_0 = \frac{1}{2} \ln \left[\frac{x^2-a^2}{1-x^2}\right]^{-\frac{1}{2}},$$

given the values of λ, a and x.

Now let $U_1 = U(+\infty)$. With this assumption, equation (4.3.5) can be

transformed into:

$$(4.3.9) \quad y_k = \frac{2}{\pi}\left[k \, \tan k^{-1}\left(\frac{2e^{2U_1} + a^2}{2e^{2U_1} + 1}\right) - h \, \tanh^{-1}\left(a\,\frac{2e^{2U_1} + 1}{2e^{2U_1} + a^2}\right)\right]$$

along the wide part of the strip, or

$$(4.3.10) \quad y_k = \frac{1}{\pi}\left[k \, \ell n \, \frac{4e^{2U_1}}{1-a^2} - h \, \ell n \, \frac{1+a}{1-a}\right] =$$

$$= \frac{2kU_1}{\pi} + \frac{1}{\pi}\left[k \, \ell n \, \frac{4k^2}{k^2-h^2} - h \, \ell n \, \frac{k+h}{k-h}\right] = \frac{2kU_1}{\pi} + A$$

where $A = \frac{1}{\pi}\left[k \, \ell n \, \frac{4k^2}{k^2-h^2} - h \, \ell n \, \frac{k+h}{k-h}\right]$.   Hence

$$(4.3.11) \quad U_1 = \frac{\pi}{2k} \, (y_k - A) .$$

exact crowding resistance

approximate crowding resistance (a small)

exact potential
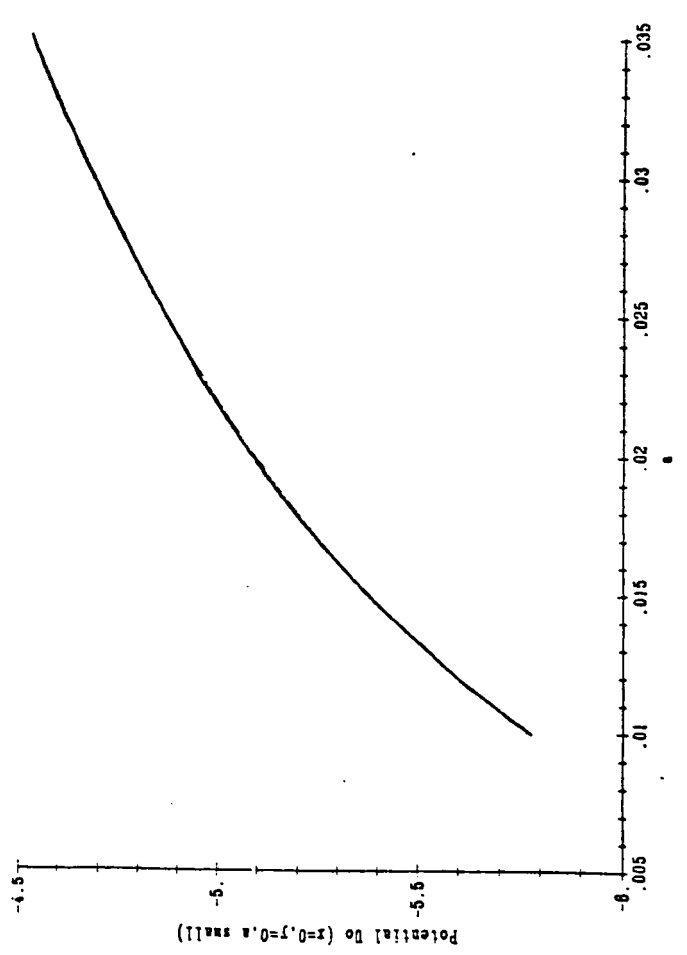
approximate potential (a small)

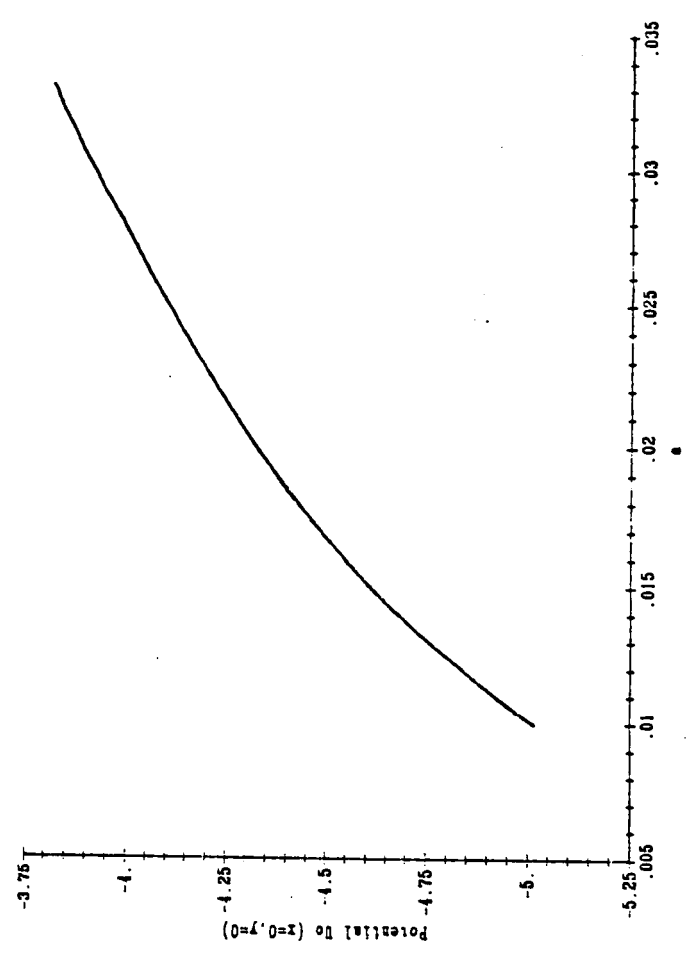| a = h/k	U_o (approx. values)	R_c (approx. values)	W	U_o (exact values)	R_c (exact values)
10.0E-3	-5.780538	1.619383	11.9966E-3	-5.016517	1.376187
11.0E-3	-5.685228	1.589048	13.1962E-3	-4.921206	1.345852
12.0E-3	-5.598217	1.561355	14.3958E-3	-4.83419	1.318158
13.0E-3	-5.518174	1.53588	15.5954E-3	-4.75414	1.292681
14.0E-3	-5.444066	1.512295	16.7950E-3	-4.680022	1.269093
15.0E-3	-5.375073	1.490339	17.9946E-3	-4.611016	1.247132
16.0E-3	-5.310534	1.469801	19.1941E-3	-4.546479	1.226594
17.0E-3	-5.249909	1.450508	20.3937E-3	-4.485836	1.207296
18.0E-3	-5.192751	1.43232	21.5932E-3	-4.428672	1.189106
19.0E-3	-5.138684	1.415116	22.7927E-3	-4.374596	1.171899
20.0E-3	-5.08739	1.398795	23.9922E-3	-4.32329	1.155574
21.0E-3	-5.0386	1.383271	25.1916E-3	-4.274498	1.140049
22.0E-3	-4.99208	1.36847	26.3911E-3	-4.227959	1.125243
23.0E-3	-4.947629	1.354328	27.5905E-3	-4.183498	1.111097
24.0E-3	-4.905069	1.340788	28.7898E-3	-4.140937	1.097557
25.0E-3	-4.864247	1.327802	29.9892E-3	-4.1001	1.084566
26.0E-3	-4.825027	1.315326	31.1886E-3	-4.06086	1.072084
27.0E-3	-4.787286	1.303221	32.3879E-3	-4.023108	1.060075
28.0E-3	-4.750918	1.291753	33.5872E-3	-3.986725	1.048503
29.0E-3	-4.715827	1.280593	34.7864E-3	-3.951625	1.03734
30.0E-3	-4.681926	1.269811	35.9856E-3	-3.917711	1.026554
31.0E-3	-4.649136	1.259383	37.1848E-3	-3.884905	1.016121
32.0E-3	-4.617387	1.249287	38.3840E-3	-3.853138	1.006019
33.0E-3	-4.586615	1.239503	39.5831E-3	-3.822353	0.9962304
34.0E-3	-4.556762	1.230011	40.7822E-3	-3.792482	0.9867331

Table 4.3.1

Finally, the total resistance of the wide part of the strip in Figure 4.3.1 not connected to the narrow one is given by:

$$(4.3.12) \quad \frac{R}{S} = \frac{1}{\pi} \left\{ \frac{\pi}{2k} (y_k - A) - U_0 \right\} = \frac{Rk}{S} + \left(-\frac{A}{2k} - U_0 \right)$$

and, since region II of Figure 4.2.1 is exactly one half of the region in Figure 4.3.1, (4.3.12) gives the total resistance also for region II, with $\frac{Rk}{S}$ the resistance of only its wide part and $-\frac{A}{2k} - U_0$ the crowding resistance.

We find:

$(4.3.13) \quad R_c = \underline{\text{Crowding resistance}} =$

$$= \frac{1}{2k\pi} \left[k \ln \frac{4h^2}{k^2 - h^2} - h \ln \frac{k+h}{k-h} \right] - U_0$$

In particular for $a \ll 1$ we get:

$$(4.3.14) \quad R_c = \frac{1}{\pi} \left[\ln 2 + \ln \frac{\lambda h}{k} + \ln \left(1 - \frac{h^2}{k^2} \right)^{\frac{1}{2}} + \frac{h^2}{k^2} \right]$$

Table (4.3.1) is a comparison between exact and approximate values of both R_c and U_0. Figure (4.3.2) illustrates the relationship between R_c, U_0 and a for the exact and approximate cases.

4. Remarks

The procedure described in 4.2 , 4.3 allows us to compute the resistance, R_S , of the source region and to express the surface potential, Φ_{S0} , at the source end of the channel as product of R_S and I . In doing

so we obviously make an approximation, which is valid at least as long as the charge-sheet model holds. We therefore obtain

(4.4.1) $\Phi_{S0} = R_S I$.

A similar procedure at the drain gives

(4.42) $V_{DS} - \Phi_{SL} = R_D I$

where R_D is the resistance of the drain region.

We can now eliminate Φ_{S0} and Φ_{SL} from the explicit formula of I_D and we obtain an equation which defines I_D implicitly.

(4.4.3) $I_D = G(I_D R_S, I_D R_D, V_{GS}, V_{BS}, \ldots)$.

This may seem a big step forward at first glance, but we would like to recall that R_S, R_D contain the crowding resistance based on the device geometry and specifically on k , the ratio between the depth of the channel and the depth of the source and drain regions. Therefore k will usually be different at the two ends and $k=0$ at the drain end when the pinch-off regime occurs. Thus the surface potential plays an important role in determining the value of k. Nevertheless it remains the fact that the doping concentration of the source (drain) region and the crowding at the two ends of the channel have made their first appearance in the drain current expression.

V. NUMERICAL RESULTS

In sections 5.1 to 5.4, we will describe the numerical algorithms which the clinic used for the evaluation of surface potentials (ϕ_{SO} and ϕ_{SL}) in the various models, followed by a numerical comparison, noting accuracy and efficiency.

Section 5.5 gives some notes on the parameter extraction procedures.

5.1 Exact Surface Potential

It should be pointed out that all the models mentioned in this report calculate ϕ_{SO} and ϕ_{SL} from the same basic one-dimensional model. The 'exact solution' is the one which uses the full 1-D equation in evaluating the surface potentials. The others use approximations to it.

The equations to be solved are those of ch. 2.2, (see 2.2.10) namely

$$5.1.1 \qquad \phi_s - V_{GS} + \alpha F(\phi_s) = 0$$

with F given by

$$5.1.2 \qquad F(x) = \left\{ e^{\beta(x - V_{BS} - \phi_n)} + e^{\beta(\phi_F + V_{BS} - x)} + \beta(x - V_{BS}) \left(e^{\beta\phi_F} - e^{-\beta\phi_F} \right) - e^{\beta\phi_F} - e^{-\beta\phi_n} \right\}^{\frac{1}{2}}$$

and

$$5.1.3 \qquad \alpha = \frac{1}{C_{ox}} \left(\frac{2qn_i\varepsilon_s}{\beta} \right)^{\frac{1}{2}} .$$

To obtain ϕ_{SO} we solve 5.1.1 with $\phi_s = \phi_{SO}$ and $\phi_n = \phi_F - V_{BS}$. For ϕ_{SL} we use $\phi_s = \phi_{SL}$ and $\phi_n = V_{DS} + \phi_F - V_{BS}$.

Newton's Method was used for the solution.

The Newton parts of the algorithms for ϕ_{SO} and ϕ_{SL} are the same, so only the general case will be explained with $\phi_s = x$.

The function whose zero we seek is

5.1.4 $\qquad G(x) = x - V_{GS} + \alpha F(x) \quad .$

The derivative is given by

5.1.5 $\qquad G'(x) = 1 + \dfrac{H(x)}{2F(x)}$

with H given by:

5.1.6 $\qquad H(x) = \beta\alpha(e^{\beta(x-V_{BS}-\phi_n)} - e^{\beta(\phi_F+V_{BS}-x)} + e^{\beta\phi_F} - 3e^{-\beta\phi_F}) \quad .$

Newton's algorithm, then, becomes:

5.1.7 $\qquad x_{k+1} = x_k - \dfrac{G(x_k)}{G'(x_k)} = x_k - \dfrac{2F(x_k)G(x_k)}{2F(x_k)+H(x_k)} \quad .$

The Fortran Statement Functions actually used are as follows:

5.1.8 $\qquad FSQ(x) = e^{\beta(x-V_{BS}-\phi_s)} + e^{\beta(\phi_F+V_{BS}-x)} + \beta(x-V_{BS})(e^{\beta\phi_F}-e^{-\beta\phi_F}) - e^{\beta\phi_F} - e^{-\beta\phi_n}$

5.1.9 $\qquad F(x) = DSQRT(FSQ(x))$

5.1.10 $\qquad G(x) = x - V_G + \alpha F(x)$

5.1.11 $\qquad H(x) = \beta(e^{\beta(x-V_{BS}-\phi_n+\ell n\alpha)} - e^{\beta(\phi_F+V_{BS}-x+\ell n\alpha)} + e^{\beta(\phi_F+\ell n\alpha)} - e^{\beta(-\phi_F+\ell n\alpha)}) \quad .$

In the function H, the $\ell n\alpha$ term in each exponential is equivalent to multiplying the expression by α. By using this form, however, the size of the exponents is reduced, minimizing the risk of overflow.

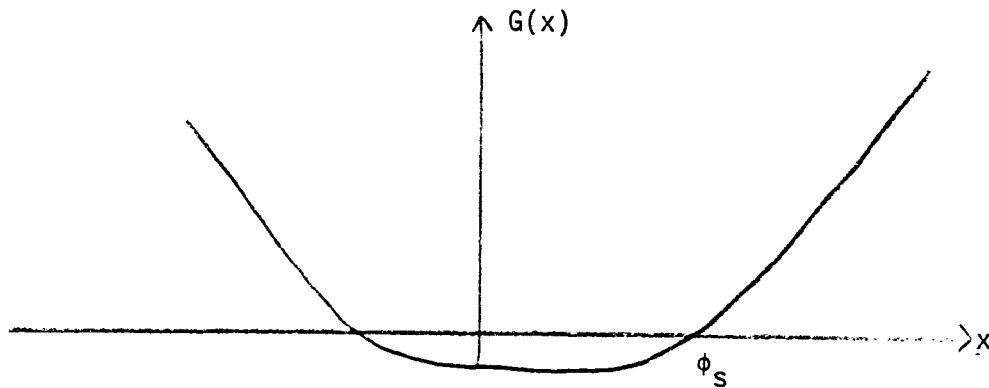The general form of the curve G(x) is given below in Figure 5.1.1.

Figure 5.1.1

The key to a successful algorithm based on Newton's Method is the initial guess for the zero. Which criteria should we use?

It was found that Newton's Method could be made to always converge for the parameter ranges given in (6.3) under the following scheme. Suppose we are given some starting value, x. Then:

5.1.12   i)   Increment x by 0.25 until FSQ(x) > 0

           ii) Increment x by 0.25 until G(x) > 0

           iii) Use Newton's Method.

The starting value for ϕ_{SO} was given as 0. ϕ_{SO} is generally positive but can be less than zero. Thus an initial value of 0 will normally converge faster since we do not need to step up through all the negative values.

The starting value for ϕ_{SL} was given as ϕ_{SO}. Although the approximation $\phi_{SL} = \phi_{SO} + V_{DS}$ might seem natural, it is not practical. When the drain is saturated, the approximation is very bad, and the starting value will be much too high. In this case, it is observed that Newton's algorithm will often converge to the wrong root - the left hand zero of G.

If the bounds on the parameter are changed substantially, then the surface potential calculations should be checked over the new range. The easiest way to do this is probably to make sure that $G'(x)$ is positive at the root.

If the algorithm does fail under different parameter ranges, there are a few things which can be changed before the need to panic becomes apparent!

Firstly, convergence of ϕ_{SO} is better guaranteed if the initial guess is set to V_{BS} instead of 0. (With the parameter bounds given in this report (5.5) convergence is guaranteed.)

With this change should also come the following: instead of incrementing x until $G(x) > 0$, do it until $G(x) > 0$ and $G'(x) > 0$. Then it will not be possible to start close to the wrong root.

Another possible reason for convergence to the wrong (left hand) root is if the increment in x is too large. Thus use a smaller increment in steps i) and ii) of the general algorithm.

The checks and changes mentioned above are not included in the parameter extraction routines as they stand, since the algorithm always converges for our physical bounds on the parameters. Each sophistication costs time, and since the programs take a good deal of that commodity already, we have kept 'extras' to a minimum.

5.2 Approximate Surface Potential (Brews)

The Brews Approximations amount to the following:

replace the functions in 5.1.8 and 5.1.11 by

5.2.1 $$FSQ(x) = e^{\beta(x-V_{BS}-\phi_n)} + \beta(x-V_{BS})e^{\beta\phi_F}$$

5.2.2 $$H(x) = \beta(e^{\beta(x-V_{BS}-\phi_n)} + \beta e^{\beta\phi_F}) \quad .$$

Then define the functions 5.1.9, 5.1.10, and the algorithm 5.1.12 is seen to converge.

There is little point in using this algorithm for Brews' surface potentials in a program, however, since the precise solution requires virtually no extra effort and convergence is the same.

A comparison of Brews' results to the precise solution is given in 5.4.

5.3 Approximate Surface Potential (Wiele)

Van de Wiele's solutions for surface potential at source and drain ends of the channel are extremely simple to calculate but unfortunately, not very accurate. A crucial first step is the determination of the inversion level associated to a particular surface potential. The condition for strong inversion is given by the relations

$$V_{GS} \gg V_T \quad \text{and jointly} \quad \phi_n + V_{BS} - \phi_F < V_1$$

5.3.1 $$V_1 = V_{GS} - 2\phi_F + \tfrac{1}{2}\lambda^2 - \lambda(\tfrac{1}{4}\lambda^2 + V_0)^{\frac{1}{2}} - \frac{2}{\beta}\ell n((\tfrac{1}{4}\lambda^2 + V_0)^{\frac{1}{2}} - \tfrac{1}{2}\lambda)$$

$$V_0 = V_{GS} - V_{BS} - \frac{1}{\beta} \qquad\qquad \lambda = (2\varepsilon_s qN_A)^{\frac{1}{2}}/C_{ox}$$

and the threshold voltage, V_T, is given recursively by,

5.3.2
$$V_T^{i+1} = V_{FB} + 2\phi_F - \tfrac{1}{2}\lambda^2 + \lambda(\tfrac{1}{4}\lambda^2 + V_t^i - V_{FB} - V_{BS} - \tfrac{1}{\beta})^{\frac{1}{2}} + \tfrac{1}{\beta}\ln\beta +$$

$$\tfrac{2}{\beta}\ln(-\tfrac{1}{2}\lambda + (\tfrac{1}{4}\lambda^2 + V_T^i - V_{FB} - V_{BS} - \tfrac{1}{\beta})^{\frac{1}{2}})$$

(see [11] eqns. (14), (13), (17)).

A simple loop is used to find the threshold voltage for each combination of V_{GS} and V_{BS}.

When the relative error between consecutive iterated values of V_T falls below $10^{-6}\%$ it is assumed to have converged to its limit. If it is determined that a condition of strong inversion exists then the Van de Wiele strong inversion approximation is used. This approximation is a recursive one and given by

5.3.3
$$\phi_{ss}^{i+1} = \phi_F + \phi_n + V_{BS} + \tfrac{1}{\beta}\ln(\beta(\tfrac{1}{\lambda})^2) + \tfrac{2}{\beta}\ln(V_{GS} - \phi_{ss}^i) \quad .$$

(See [11] eqn (9)).

Here again, a relative error of less than $10^{-6}\%$ between iterations is taken as proof of convergence.

If the conditions for strong inversion are not met, the weak inversion approximation is used. This is given simply and nonrecursively by

5.3.4
$$\phi_{sw} = V_{GS} + \tfrac{1}{2}\lambda^2 - \lambda(\tfrac{1}{4}\lambda^2 + V_0)^{\frac{1}{2}} \quad .$$

(See [11], eqn.(12)).

5.4 Comments (numerical comparison)

As Van de Wiele uses the same formulae for the surface potential at
the source and drain ends of the channel we may use the same approach for
calculating either one. The only difference between source and drain end
of the channel lies in our value for ϕ_n. At the source end we take $\phi_n =$
$\phi_F - V_{BS}$ whereas at the drain end we take $\phi_n = \phi_F - V_{BS} + V_{DS}$. The Van
de Wiele model has the advantage of being computationally direct, involving
limited logical checks and only simple loops. Unfortunately, this simplicity
is at the expense of accuracy. Two runs were made, each for a different set
of parameters. For run 1: $\lambda = 2.312$, $\phi_F = 4$, $C_{ox} = 6.9 \times 10^{-8}$. For run 2:
$\lambda = .4042$, $\phi_F = .35$, $C_{ox} = 23 \times 10^{-8}$. ϕ_{S0} and ϕ_{SL} were calculated through
the following range of voltages: $2 \leq V_{GS} \leq 5$, $V_{BS} = 0$ and $-2 \geq V_{BS} \geq -5$,
$1 \leq V_{DS} \leq 5$.

Each run compared the potentials calculated by the Brews and the Van de
Wiele models with the potentials calculated by the exact, Pao-Sah model, for
each possible set of voltages, and expressed the difference in terms of a
relative error. For the accurate measurement of error, the height of ϕ_s
above V_{BS} must be taken into account. Thus the expression for relative
error becomes: $100 \times (\phi_s (EXACT) - \phi_s (APPROX))/(\phi_s (EXACT) - V_{BS})$.

In the first run, Brews' approximation yielded an RMS error of .3% and
.5% for ϕ_{S0} and ϕ_{SL} respectively. At no time did the error rise above .7%/1.6%.
The Van de Wiele approximation was not quite as good yielding an RMS error of
1.4% and .2% with maximum errors of 5.3%/1.2%. For the second run, Brews showed
0% RMS error in ϕ_{S0} and ϕ_{SL}. There was only one instance of non zero error
which was an insignificant .1%. Van de Wiele returned 1.1% and 3.9% RMS errors

with individual cases as high as 2.4% and 7.7%. Clearly then for the purposes of parameter extraction, the Brews approximation shows itself to be an excellent one with almost insignificant error. The Van de Wiele approximation, while not as good, is still reasonable for $\lambda = 2.312$. However, for small λ ($\lambda = .4042$) errors become noticeable and its use becomes questionable.

5.5 Parameter Extractions

The parameters used by last year's clinic with the Brews model have been modified by the clinic. Previously it was the case that 2 of the parameters each contained two required quantities. Namely

$$p_1 = p_1(\phi_F)$$

5.5.1 $\qquad p_2 = p_2(\phi_F, C_{ox})$

$$p_5 = p_5(W/L, C_{ox}) \quad .$$

Since ϕ_F, C_{ox}, and W/L are the real quantities we wish to find, we have set the new parameters to be:

$$p_1 = \phi_F$$

5.5.2 $\qquad p_2 = C_{ox}$

$$p_5 = W/L \quad .$$

What bounds should be put on the paramters? From physical considerations, we have the following:

5.5.3 $\qquad 0.29 \leq \phi_F \leq 0.41V$ corresponding to $10^{15} \leq N_A \leq 10^{17}$,

$\qquad -0.95 \leq V_{FB} \leq -0.8V$ for n-channel ,

$\qquad -0.3 \leq V_{FB} \leq -0.2V$ for p-channel .

W   and   L   are given for each device. Acceptable bounds for   W/L
would be 10% to either side of the given value.

For the Brews and Van de Wiele models, the full one-dimensional solution
for surface potentials is used. Also, we have coded Van de Wiele's approxi-
mate solutions in the hope that they may be more computationally efficient.
A comparison of the various surface potential calculations was given in 5.4.

6. CONCLUSIONS

The new formulation of drain current given in (3.4) is, we feel, more acceptable than those previously derived. If an approximation of x_i could be found in region A, then it would be complete. As it stands, however, the importance of such a correction is not known. Tests should be carried out comparing the approximations for Q_n with numerically computed values--this should also be done for the Van de Wiele model.

What is it about this model which is more acceptable?

Firstly it includes the contribution of current from the pinched off part of the device which is not seen in any of the other models we have looked at.

Secondly, in the Brews and Van de Wiele models, the result $Q_D = K\{\beta(\phi_s - V_{BS}) - 1)\}^{\frac{1}{2}}$ is used for the depletion charge. This result is the same as the clinic's model in region B, but look at how they calculated this value. Firstly, they assume that all the charge not due to electrons is due directly to the doping, N_A, and that the depleted region is uniform to a depth W, beyond which charge neutrality exists. Thus they solve the equation $\varepsilon_s \, d^2\phi/dx^2 = q \, N_A$. In fact, as we go down into the bulk of the device, the hole charge, p, increases con-tinuously and only asymptotically to the value N_A, which gives charge neutrality. The boundary conditions they use at the surface are those of the full 1-D Poisson. Hence this approach would seem to neglect the sharp increase in the actual potential near the surface caused by the inversion layer electron charge. The clinic has not been able to justify the use of this approach for finding Q_D.

In our model we allow all the charge distributions to be continuous, and do not lose the inversion layer structure.

Brews claims that his model is valid in all regimes of operation. Numerically, this is not what we find. By using parameter extraction, we can get a good fit to wide ranges of data. However, there are certain combinations of voltages which <u>without</u> <u>fail</u> cause large errors. Notably $V_{GS} = 2$, $V_{BS} = -3,-4,-5$.

The departure of the model from reality in these conditions can be by 30 or 40% compared to less than 5% for most all the other voltages (for one given fit to data). It would thus seem reasonable to assume that the model is having trouble fitting to these particular applied voltages. The reason for this may be that his model uses a single formula for Q_n whatever the operating conditions at any point in the device. The clinic, however, splits the device into 3 regions with different approximations in each.

What is required now is a thorough testing of the various forms of Q_n which are used in the two models, as well as an attempt to find x_i in region A as an integrable function.

All the models mentioned in this report are based on the Pao-Sah formulation of drain current. Typically, instead of integrating directly to find Q_n, the route using $Q_{sc} = Q_n + Q_D$ is taken.

As has been noted previously, the Pao-Sah double integral formula is found to be highly accurate for long-channel MOSFETs. For short-channel devices, accuracy is not guaranteed.

The main inaccuracy in this model is due to its main feature: namely the integration of Poisson's equation. In order to do this integration, two assumptions are needed: $\phi_n = \phi_n(y)$ and $\partial^2\phi/\partial y^2 \ll \partial^2\phi/\partial x^2$. The effect of these assumptions is to make the model a combination of two uncoupled one-dimensional models, rather than a true two-dimensional model.

What is needed now is to start with a model based on Pao-Sah, and to extend it to something which is "more two-dimensional". Part of this approach should be in the source-drain modeling. Thus ϕ_{SO} and ϕ_{SL} are no longer calculated from the one-dimensional Poisson, but from full solutions to the source and drain equations. The clinic has analysed much of the large amount of work done in this area. We have chosen the approaches which are most mathematically sound (yet not too complex to be unworkable) and presented them as a full and concise reference for future attempts to include source and drain effects in a drain current model.

Along with this approach, we need to add some y dependence to the solution of Poisson's equation. This is particularly important at the source and drain where irregular device geometry and rapid changes in carrier concentrations along the channel (e.g., caused by pinch-off) can make the one-dimensional approximation very unrepresentative of the true situation.

A clear understanding of the tricks and techniques used in one-dimensional modeling is paramount before attempting the step to quasi-two-dimensionality.

The main achievement of this Clinic is that we have clarified the approaches commonly used in one-dimensional modeling, consolidated much of the large amount of work done on source and drain modeling, and possibly produced an optimal one-dimensional model for MOSFET current. Initially, we had planned to produce a two-dimensional model, but the lack of what we considered to be a fully justified 1-D formulation led us, instead, to concentrate on this, thus producing a good basis for future mathematical modeling in this area.

For the computing, we have produced efficient, accurate algorithms for the solution of surface potentials. These have been incorporated into parameter extraction programs for the Brews and Van de Wiele models.

APPENDIX   I

NOTATION AND SYMBOLS

The notation and symbols detailed below have been used exclusively throughout the report.

L	Channel Length
L_e	Effective channel length
W	Width of the device
$x_i(y)$	Depth of the inversion region
$D(y)$	Depth of the depletion region
μ_n	Electron mobility
μ_{eff}	Effective electron mobility
C_{ox}	Oxide layer capacitance per unit area
n_i	Intrinsic Carrier Concentration
N_A	Dopant ion concentration (acceptors)
Q_n	Charge density due to free electrons in the inversion layer
Q_s	Total space charge density
Q_D	Depletion region charge
J	y component of current density in the channel
J_n	y component of electron current density in the channel
n	Carrier density of electrons
p	Carrier density of holes
$\phi(x,y)$	The potential measured relative to the source
$\phi_s(y)$	ϕ at $x = 0$, the surface potential
ϕ_{s0}	$\phi_s(0)$ i.e., surface potential at the source

ϕ_{SL} $\quad\quad$ $\phi_S(L)$ i.e., surface potential at the drain

ϕ_n $\quad\quad$ Electron quasi Fermi potential

ϕ_p $\quad\quad$ Hole quasi Fermi potential

ϕ_F $\quad\quad$ $= \beta^{-1}\ln(\frac{N_A}{n_i})$, bulk Fermi potential

ε_0 $\quad\quad$ Permittivity of free space

κ_s $\quad\quad$ Dielectric constant for silicon

ε_s $\quad\quad$ $= \kappa_s\varepsilon_0$

k_{ox} $\quad\quad$ Dielectric constant for oxide

k $\quad\quad$ Boltzman constant

T $\quad\quad$ Absolute temperature $/°K$

β $\quad\quad$ $= q/kT$

L_D $\quad\quad$ $= (\varepsilon_s/(n_i q\beta))^{\frac{1}{2}}$: Intrinsic Debye Length

L_B $\quad\quad$ $= (\varepsilon_s/N_A q\beta))^{\frac{1}{2}}$: Debye Length (bulk)

α $\quad\quad$ $= \sqrt{2}qN_A L_B C_{ox}$

σ $\quad\quad$ $= 2\varepsilon_s qN_A/C_{ox}$

V_{BS} $\quad\quad$ body bias relative to the source

V_{DS} $\quad\quad$ drain bias relative to the source

V_{GS} $\quad\quad$ gate bias relative to the source less the flat band voltage, V_{FB}

V_{GB} $\quad\quad$ gate bias relative to the body less V_{FB}

V_{FB} $\quad\quad$ Flatband voltage

t_{ox} $\quad\quad$ Thickness of the oxide layer

λ $\quad\quad$ $= (\sigma_m \rho_c)^{-1}$ where ρ_c is contact resistivity, σ_m is material conductivity

APPENDIX II

NOTATION AND SYMBOLS OF VARIOUS MODELS

This section is a translation for changing expressions found in some of the papers we have used into the clinic's standard notation. It should be noted that the source to substrate bias is zero in Pao-Sah [6] and Brews [2]. Thus it is only valid to set $V_{BS} = 0$ when comparing these to the other three papers.

Clinic	Pao-Sah [6]	Van de Wiele [11]	Brews [3]	Brews [2]
V_{BS}	0	$V_B - V_S$	$-V_{BS}$	0
V_{GS}	$U_G^!/\beta$	$V_G - V_S - V_{FB}$	$V_G - V_{BS}$ or V_{GS}	V_G
V_{DS}	U_D/β	$V_D - V_S$	V_{DS}	V_D
0	0	V_S	0	0
ϕ	U/β	$\phi - V_S$	$\phi - V_{BS}$	ϕ
ϕ_s	U_S/β	$\phi_s - V_S$	$\phi - V_{BS}$	ϕ_s
ϕ_F	U_F/β	ϕ_F	ϕ_F	ϕ_B
$\phi_n + V_{BS}$	$(\xi+U_F)/\beta$	$V(y) + \phi_F$	$\phi_{F_n} - V_{BS}$	ϕ_f
x	x	x	y	x
y	y	y	x	y
Q_{SC}	--	Q_{SC}	Q_S	Q_S
Q_D	--	Q_D	--	--
Q_n	--	Q_N	N_I	N_I

REFERENCES

[1] G. Baccarani, et. al. IEE J. Solid St. and Electron Dev. 2, 62, 1978.

[2] J.Brews. Solid State Electronics, 1978, Vol. 21, pp. 345-355.

[3] J. Brews. Physics of the MOS transistor, 1980, Report to Bell Labs.

[4] R. Gribben, M. Martelli. Optimal Parameter Extraction for the Brews Charge Sheet MOSFET Model.

[5] H. Morris, R. Everson. J.P.L. Report of Summer, 1984.

[6] H. C. Pao, C. T. Sah. Solid State Electronics, 1966, Vol. 9, pp. 927-937.

[7] R. Pierret, J. Shields. Solid State Electronics, 1983, Vol. 26, pp. 143-147.

[8] R. Plonsey, R. E. Collin. Principles and Applications of Electromagnetic Fields, McGraw-Hill Book Company, Inc., 1961, pp. 171-177.

[9] W. R. Smythe. Static and Dynamic Electricity, II Ed., McGraw-Hill Book Company, Inc., 1950, pp. 235-237.

[10] S. M. Sze. Physics of Semiconductor Devices, 1981, II Ed., Wiley-Inter-Science.

[11] F. Van De Wiele. Solid State Electronics, 1979, Vol. 22, pp. 991-997.

[12] M. Walker. The Schwarz-Christoffel Transformation and its Applications: a simple exposition. (Formerly titled: Conjugate Functions for Engineers) New York, Dover, 1964.